



12-2014

# Localization of chemoreceptors in *Azospirillum brasiliense*.

Anastasia Aksenova

University of Tennessee - Knoxville, [aaksenov@vols.utk.edu](mailto:aaksenov@vols.utk.edu)

---

## Recommended Citation

Aksenova, Anastasia, "Localization of chemoreceptors in *Azospirillum brasiliense*.. " Master's Thesis, University of Tennessee, 2014.  
[https://trace.tennessee.edu/utk\\_gradthes/3135](https://trace.tennessee.edu/utk_gradthes/3135)

This Thesis is brought to you for free and open access by the Graduate School at Trace: Tennessee Research and Creative Exchange. It has been accepted for inclusion in Masters Theses by an authorized administrator of Trace: Tennessee Research and Creative Exchange. For more information, please contact [trace@utk.edu](mailto:trace@utk.edu).

To the Graduate Council:

I am submitting herewith a thesis written by Anastasia Aksenova entitled "Localization of chemoreceptors in *Azospirillum brasilense*." I have examined the final electronic copy of this thesis for form and content and recommend that it be accepted in partial fulfillment of the requirements for the degree of Master of Science, with a major in Biochemistry and Cellular and Molecular Biology.

Gladys Alexandre, Major Professor

We have read this thesis and recommend its acceptance:

Brad Binder, Andreas Nebenfuehr, Jennifer Morrell-Falvey

Accepted for the Council:

Carolyn R. Hodges

Vice Provost and Dean of the Graduate School

(Original signatures are on file with official student records.)

---

Localization of chemoreceptors in *Azospirillum brasilense*.

A Thesis Presented for the  
Master of Science  
Degree  
The University of Tennessee, Knoxville

Anastasia Aksenova  
December 2014

Copyright © 2014 by Anastasia De Cerqueira  
All rights reserved.

## **ACKNOWLEDGEMENTS**

This research project would not have been possible without the support of many people. First of all, I would like to express my gratitude to my advisor, Dr. Gladys Alexandre who was very helpful and offered valuable assistance, support, and guidance (and the most valuable funding for the project). Also, I would like to show my gratitude to members of my committee, Dr. Andreas Nebenfuehr, Dr. Jennifer Morrell-Falvey, and Dr. Brad Binder for their time and valuable input on my project. Finally, I would like to acknowledge all the members of the Alexandre lab, and especially the undergraduate (Angela Yu and Cody Burton) and graduate (Jessica Gullett and Lindsey O'Neal) students who helped me working on my project and provided excellent technical support.

This thesis would not have been possible without the support of my beloved family members, especially my husband, my wonderful in-laws, my mom, and my friends.

## ABSTRACT

In order to ensure their survival, bacteria must sense and adapt to a variety of environmental signals. Motile bacteria are able to orient their movement in a chemical gradient by chemotaxis. During chemotaxis, environmental signals are detected by chemotaxis receptors and are propagated via a signal transduction cascade to affect bacterial motility. In a model organism *Escherichia coli*, chemotaxis receptors, also called MCPs (for methyl-accepting chemotaxis proteins) sense changes in concentration gradients by making temporal comparisons about the chemical composition of their surroundings. Decreased attractant concentration or increased repellent concentration results in conformational changes in the MCPs that culminate in autophosphorylation of histidine kinase CheA that in turn phosphorylates response regulator CheY. Phosphorylated CheY interacts with flagellar rotor switch protein FliM and causes it to switch direction of rotation.

In *E. coli*, MCPs form mixed trimers-of-receptor dimers. Together with CheA and CheW proteins they further organize into large patches at the cell poles called arrays. This architecture is important for signal amplification and propagation and is universally conserved among many bacterial species. In contrast to *E. coli*, nitrogen-fixing soil bacteria, *Azospirillum brasilense*, encode four chemotaxis pathways and 41 MCPs. Previous work shows both Che1 and Che4 contribute to chemotaxis and aerotaxis implying that signals detected by chemotactic receptors must be integrated to generate a coordinated motility response. In this work, fluorescent microscopy imaging studies of some *A. brasilense* MCPs (Tlp1, Tlp2, Tlp4a, and AerC) in various mutant backgrounds demonstrate their localization in respect to each other and to CheA1 and CheA4 proteins.

# TABLE OF CONTENTS

|  |    |
|--|----|
| CHAPTER I. Introduction .....  | 1  |
| Structure of bacterial chemoreceptors. ....  | 2  |
| Chemotaxis in <i>E. coli</i> . ....  | 4  |
| Organization of chemoreceptors in <i>E. coli</i> . ....  | 6  |
| Organization of chemoreceptors in other bacteria. ....   | 10 |
| Chemotaxis in <i>Azospirillum brasilense</i> is controlled by multiple Che pathways. ....  | 12 |
| CHAPTER II. Materials and Methods.....   | 17 |
| Strains and growth conditions.....   | 17 |
| Plasmids/strains construction and fluorescence microscopy. ....  | 20 |
| Evaluating protein expression using Western blotting. ....   | 21 |
| Bacteria-Two Hybrid Assay (BACTH). ....  | 22 |
| CHAPTER III. Results.....  | 25 |
| CheA4 is required for polar localization of Tlp4a-YFP and Tlp1-YFP fluorescent foci. ....  | 25 |
| <i>In vivo</i> interactions of chemoreceptors with chemotaxis proteins in Che1 and Che4 pathways<br>evaluated by Bacteria-Two Hybrid Assay. .... | 33 |
| Relative subcellular localization of chemoreceptors. ....  | 38 |
| <i>In vivo</i> interactions of chemoreceptors with one another evaluated by Bacteria-Two Hybrid<br>Assay.....                                    | 48 |
| CHAPTER IV. Discussion.....  | 50 |
| LIST OF REFERENCES .....   | 55 |
| VITA .....   | 61 |

## LIST OF TABLES

|  |    |
|--|----|
| Table 1. Summary of measurements of 13 different bacterial species obtained by cryo-ET. .... | 11 |
| Table 2. Plasmids and strains used in this study. ....                                       | 19 |
| Table 3. Primers .....   | 23 |
| Table 4. Colony PCR conditions. ....   | 24 |



## LIST OF FIGURES

|  |    |
|--|----|
| Figure 1. Schematic representation of MCP cytoplasmic domain features as revealed by a multiple sequence alignment of C-terminal domains. ....   | 3  |
| Figure 2. The chemotaxis signaling pathway in <i>E. coli</i> . ....  | 5  |
| Figure 3. Top-view of the arrangement of the array components. ....  | 8  |
| Figure 4. <i>Azospirillum brasilense</i> has four chemotaxis-like operons. ....  | 13 |
| Figure 5. CheA4 is required for proper localization of chemoreceptors. ....  | 28 |
| Figure 6. Relative fluorescence intensity and total cell fluorescence of Tlp1-YFP and Tlp4a-YFP is decreased in $\Delta cheA4$ and $\Delta cheA1 \Delta cheA4$ backgrounds compared to the wild type. .... | 29 |
| Figure 7. Tlp1-YFP and Tlp4a-YFP fluorescent foci appear mislocalized in the $\Delta cheA4$ and $\Delta cheA1 \Delta cheA4$ backgrounds. ....  | 30 |
| Figure 8. Cellular levels of Tlp1-YFP and Tlp4a-YFP expressed from pRH005 plasmid. ....  | 32 |
| Figure 9. BACTH analysis testing for interactions of chemoreceptors Tlp1, Tlp4a, and AerC with CheA1, CheA4, CheW1, CheW4 chemotaxis proteins and with one another. ....                                   | 36 |
| Figure 10. Graphical representation of BACTH assay results depicting interactions of the chemoreceptors with chemotaxis proteins in the CheA1 and CheA4 pathways. ....                                     | 38 |
| Figure 11. Localization of chemoreceptors in respect to one another. ....  | 40 |
| Figure 12. Relative fluorescence intensity of Tlp4a-YFP and Tlp1-YFP is decreased in $\Delta aerC$ background compared to the wild type. ....  | 43 |
| Figure 13. Cellular levels of Tlp1-YFP and Tlp4a-YFP expressed from pRH005 plasmid. ....   | 44 |
| Figure 14. Relative fluorescence intensity of AerC-YFP is decreased in $\Delta tlp1$ background compared to the $\Delta aerC$ background. ....   | 45 |
| Figure 15. Localization of Tlp1-YFP and Tlp2-YFP is affected in the $\Delta aerC$ background while Tlp4a-YFP localizes to the cell pole irrespective of the background. ....                               | 46 |
| Figure 16. Tlp1-YFP and Tlp2-YFP fluorescent foci are lateral in the $\Delta aerC$ background while Tlp4a-YFP foci localize to the cell pole(s) in all backgrounds. ....                                   | 47 |
| Figure 17. Graphical representation of BACTH assay results depicting interactions of the chemoreceptors with one another. ....   | 49 |
| Figure 18. Model of chemoreceptors clusters organization in <i>A. brasilense</i> . ....  | 54 |

## CHAPTER I. Introduction

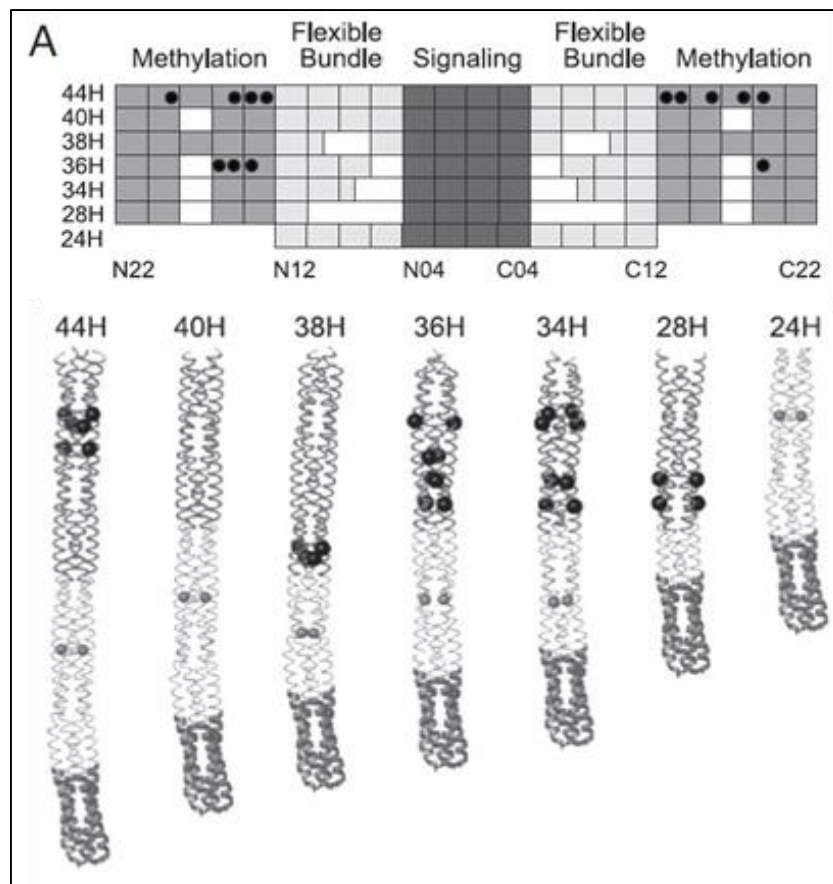
In order to ensure their survival, bacteria must sense and adapt to a variety of environmental signals and to be able to avoid harmful environments and to seek beneficial ones. Movement of bacteria towards chemical attractants and away from chemical repellants is called chemotaxis. Chemotaxis (taxis in gradients of chemical effectors) is one of the most common taxis responses in bacteria but other forms of taxis include aerotaxis (movement in oxygen gradient), phototaxis (movement in gradient of light), and pH taxis (movement in pH gradient) (Wadhams and Armitage, 2004). Chemotaxis in bacteria can be described as a "random biased walk": motile bacteria set off swimming in one direction, and if conditions get better they keep moving ("run") in that direction. If conditions get worse (decreased attractant concentration or increased repellent concentration), bacteria tend to "tumble", randomly being reoriented by Brownian motion to swim in a new direction.

In order to sense changes in the environment and adapt to them, bacteria, like the model organism *Escherichia coli* use a dedicated signal transduction system comprised of five chemoreceptors and six chemotaxis proteins (CheA, CheW, CheY, CheZ, CheR, and CheB) encoded within a single operon (Silverman and Simon, 1976; Francis *et al.*, 2004; Wadhams and Armitage, 2004). This is in contrast to many soil and aquatic bacteria, the majority of which contain multiple chemotaxis operons and a large number of receptors (Porter *et al.*, 2011). These features allowed for *E. coli* to become a model organism for studying chemotaxis signal transduction.

## **Structure of bacterial chemoreceptors.**

In *E. coli*, chemotaxis receptors, also called MCPs (for methyl-accepting chemotaxis proteins) sense changes in concentration gradients by making temporal comparisons about the chemical composition of their surroundings (Sourjik and Wingreen, 2012). A functional unit of chemoreceptors is a helical homodimer. Typically, each monomer in a dimer contains a ligand binding region (LBR) at the N-terminus, exposed on the periplasmic side of the membrane and flanked by two transmembrane domains, and a C-terminal signaling region located in the cytoplasm. A typical *E. coli* chemoreceptor LBR is a four-helix bundle structure arranged in parallel that, in a dimer, forms a cluster of eight helices where ligands bind (Milburn *et al.*, 1991). The LBRs vary greatly in sequence reflecting their role in binding different compounds (Zhulin, 2001). It is noteworthy that 88.7% of LBRs are un-annotated in the SMART database (a database used for the identification, annotation, and prediction of architecture of protein domains; Letunic *et al.*, 2011), suggesting that they are novel domains for which a sensory specificity cannot be predicted from sequence analysis alone (Wuichet *et al.*, 2010). MCPs can be further classified by their topology type into 6 different classes with Class I being the most abundant. The signaling region of a chemotaxis receptor is highly conserved among MCPs as it interacts with components of the chemotaxis signaling pathway in the cytoplasm (Alexander and Zhulin, 2007). This region consists of a methylation, flexible bundle domain critical for signal transduction, as well as signaling sub-domains implicated in CheA and CheW binding (Falke and Hazelbauer, 2001; Zhulin, 2001; Alexander and Zhulin, 2007). Sequence alignment of 1,915 MCPs from 152 genomes of Bacteria and Archaea showed that MCPs could be organized into 7 major classes based on the sequence conservation and the presence of symmetric seven amino

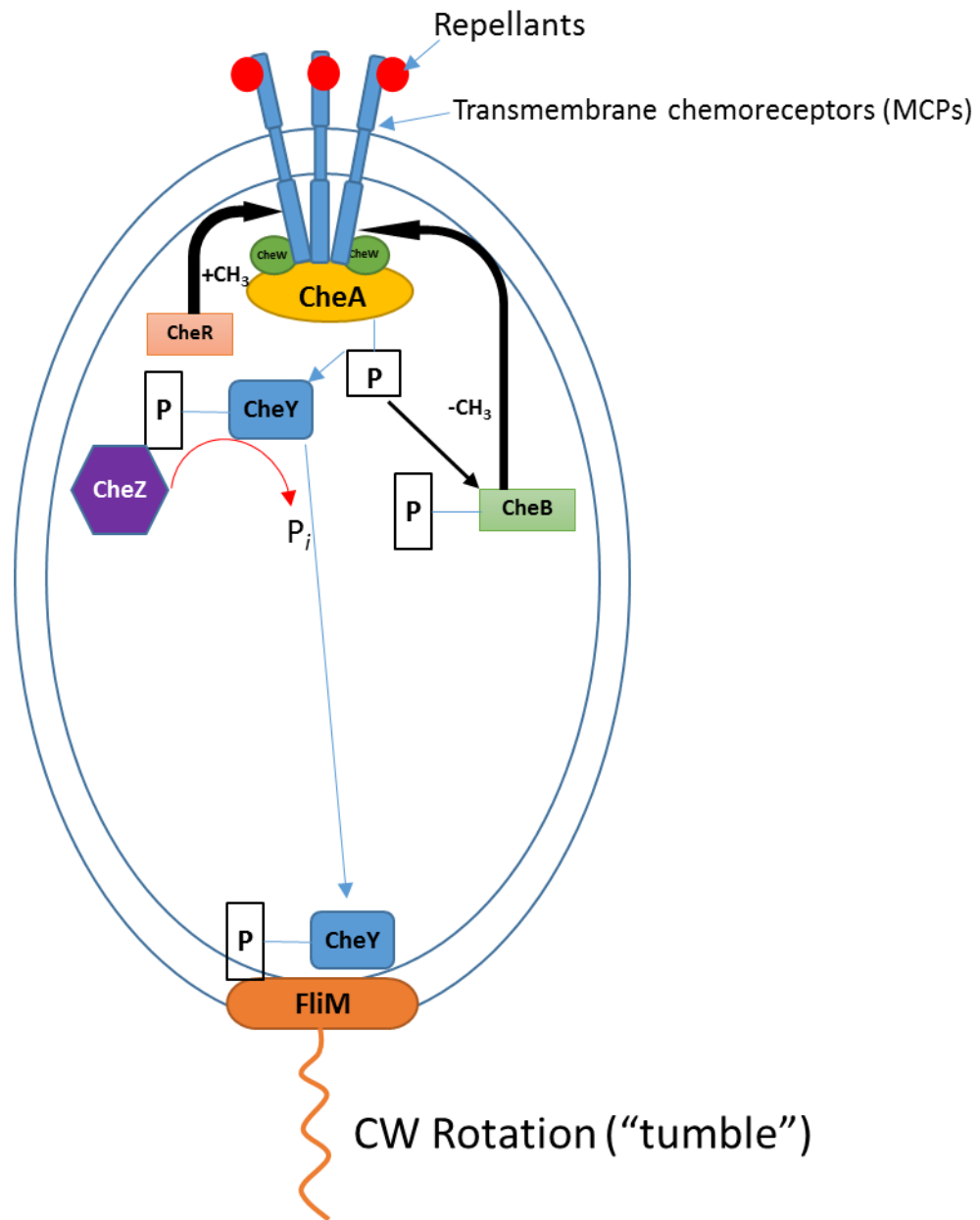
acid-long insertions and deletions, corresponding to two  $\alpha$ -helical turns and defined as heptads (H) (Figure 1). In addition, sequence conservation in the signaling domain led to the proposition that all chemoreceptors form dimers, regardless of the structural class they belong to (Wuichet *et al.*, 2010).



**Figure 1. Schematic representation of MCP cytoplasmic domain features as revealed by a multiple sequence alignment of C-terminal domains. The signaling subdomain is shown in dark thick ribbons. (Alexander and Zhulin, 2007).**

## **Chemotaxis in *E. coli*.**

In *E. coli*, binding of attractants to LBR of MCPs results in the piston-like movement of the transmembrane region towards the cytoplasm which in turn leads to signal conversion and propagation (Parkinson *et al.*, 2010). In the cytoplasm, the C-terminal signaling regions of MCPs interact with a histidine kinase CheA and a coupling protein CheW to form ternary complexes where transduction of the chemotaxis signal is initiated (Maddock and Shapiro, 1993; Studdert and Parkinson, 2004). CheA is a dimeric protein consisting of five structural domains (P1-P5): P1 is a histidine phosphotransfer domain that gets phosphorylated by the P4 kinase domain, P2 binds the response regulator CheY and the methylesterase CheB, P3 is the domain responsible for dimerization, and P5 is a CheW-like domain that binds CheW and the tips of the chemoreceptors (McNally and Matsumura, 1991; Gegner *et al.*, 1992). Signal propagation down the length of the MCPs results in conformational changes in various domains culminating in ophosphorylation of CheA. CheA, in turn, phosphorylates its response regulator CheY. Phosphorylated CheY (CheY-P) gets released from the MCP/CheA/CheW cluster and interacts with the flagellar motor switch protein FliM which causes it to switch the direction of flagellar rotation (Falke *et al.*, 1997). The probability of switching the direction of flagellar rotation increases with increasing number of CheY-Ps binding to FliM subunits (Bai *et al.*, 2010). The signaling stops when CheY-P becomes dephosphorylated by its dedicated phosphatase, CheZ.



**Figure 2.** The chemotaxis signaling pathway in *E. coli*.

Counter-clockwise rotation of flagellar motor results in the forward movement, while clockwise rotation of one or more flagella motors causes bacteria to tumble (Welch *et al.*, 1993). Binding of attractants and repellants to the LBR of chemoreceptors allows them to sense current conditions while methylation/demethylation of specific residues located in the cytoplasmic region of chemoreceptors, by the combined activities of CheR (methyltransferase) and CheB (methyl-esterase), mediates the adaptation response of the receptors by readjusting their sensitivity upon sensing a cue (Figure 2, Wadhams and Armitage, 2004). For example, when attractants concentration decreases, CheA phosphorylates Che-Y (see above) and methyl-esterase CheB (CheB-P). CheB-P counteracts the constitutive activity of CheR and removes methyl groups from specific glutamate residues in the cytoplasmic domains of the MCPs, an event that eventually decreases CheA autophosphorylation. As the concentration of CheY-P decreases cells become smoother swimming, i.e. tumble less frequently. Differential methylation of chemoreceptors restores the movement bias to the pre-stimulus level and provides the cells with a short term “memory”, allowing cells to compare current conditions to the previous ones.

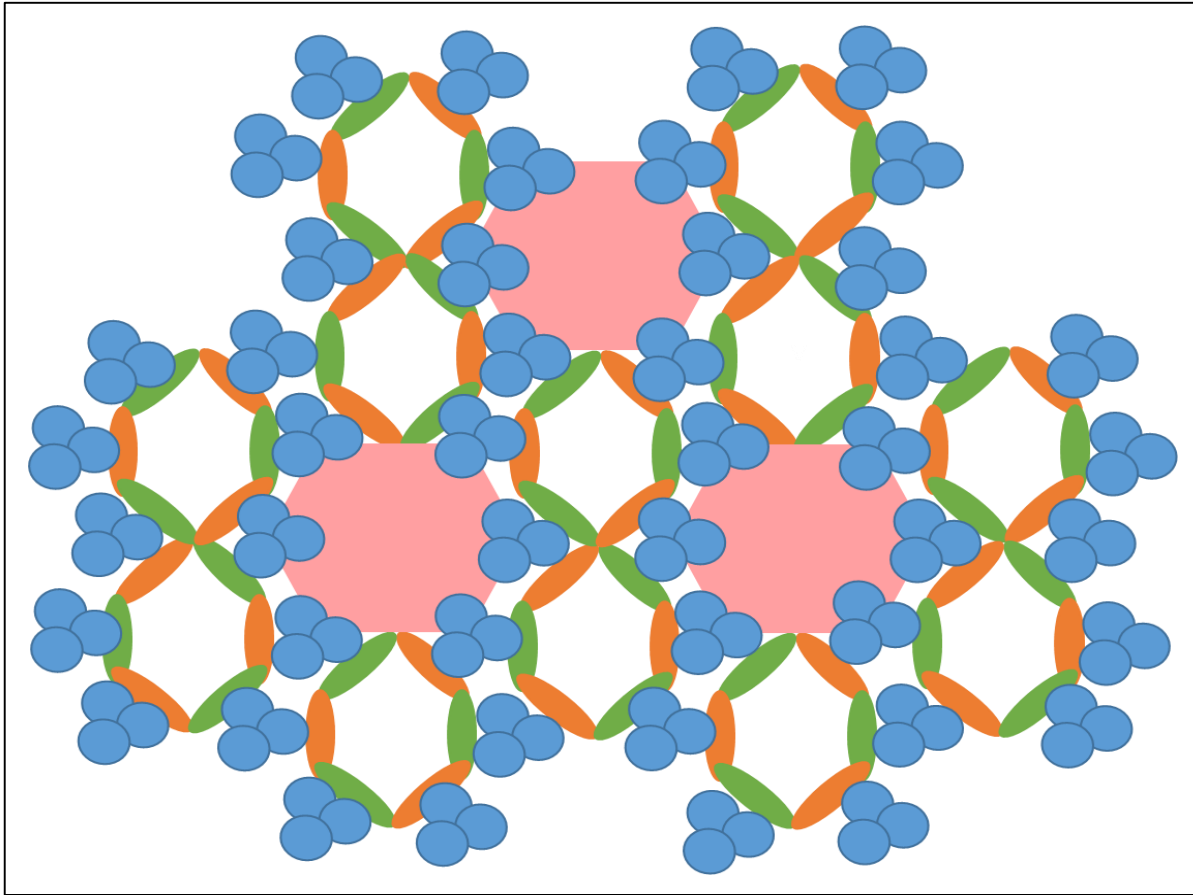
### **Organization of chemoreceptors in *E. coli*.**

*E. coli* has four canonical MCPs (Tsr – senses serine, Tar – senses maltose and aspartate, Tap – senses dipeptides and pyrimidines, and Trg – senses galactose and ribose) and an MCP-like receptor Aer for redox potential (Silverman and Simon, 1976; Rebbapragada *et al.*, 1997; Bibikov *et al.*, 2004). All five of these receptors form mixed clusters and localize to the cell poles along with CheA and CheW proteins to form large patches (~250 nm average diameter), as evidenced by immunofluorescent microscopy, immunogold labeling, and cryoelectron tomography (cryo-ET) studies (Maddock and Shapiro, 1993; Sourjik and Berg, 2002; Briegel *et*

*al.*, 2009). While the majority of the patches (80%) localizes to the cell pole and remains mobile, the non-polar patches are steady and form next to future division sites (Thiem *et al.*, 2007). Experimental evidence and mathematical modeling indicate that allosteric interactions among receptors in the patches allow for signal amplification up to 36-fold, implying that one receptor may interact with dozens of CheA kinase molecules (Sourjik and Berg, 2002). Signal amplification is critical to chemotaxis, as it enables bacteria to sense and quickly respond to the smallest changes in their environment.

Cryo-ET of *E. coli* mini-cells revealed that receptors form a hexagonal lattice with a 12 nm spacing, each hexagon representing a trimer-of-chemoreceptor dimers (Liu *et al.*, 2012; Briegel *et al.*, 2013). The neighboring trimers are connected by a continuous density layer comprised of CheA and CheW proteins, forming large patches called receptor arrays (Figure 3). These patches are stabilized by the interactions between CheW and the P5 domain of CheA, as well as between the cytoplasmic tips of MCPs and the P3 domain of CheA (Park *et al.*, 2006; Liu *et al.*, 2012). Six core complexes that consist of one trimer-of-dimers and CheA and CheW proteins form a ring with a hole in the middle that could be filled with the CheW proteins interacting with the tips of MCPs, further stabilizing the array (Liu *et al.*, 2012).





**Figure 3. Top-view of the arrangement of the array components.** Receptors trimers-of-dimers (blue) interact with CheAs (green) and CheWs (orange) to form extended lattice structures called arrays. CheA-empty hexagons are colored pink.

Fluorescent microscopy studies of *E. coli* chemoreceptors revealed that in the absence of CheA and CheW proteins, receptors localization appeared to be more diffuse with caps or multiple small clusters at the pole instead of the compact clusters seen as single foci at the cell poles of wild type cells (Kentner *et al.*, 2006). These evidence suggest that CheA and CheW proteins are not required for cluster formation but assist in stabilization of the clusters in a compact form. In addition, cross-linking studies demonstrated that chemoreceptors of different types form mixed trimers *in vivo*, even in the absence of CheA and CheW, with their composition depending on the relative expression of the receptors (Studdert and Parkinson, 2003).

Recent cryo-ET studies of the *E. coli* Tar chemoreceptor revealed a model for chemoreceptor array assembly (Briegel *et al.*, 2014). The authors propose that, as the receptors are synthesized and inserted into the membrane, they quickly dimerize to form trimers-of-dimers. CheA dimers, in the cytoplasm, then capture the newly assembled trimers-of-dimers to form six-receptor functional units that either attach to existing arrays through CheW or link together. Consistent with this model, *in vitro* studies in which membranes containing receptors were incubated with purified CheA and CheW revealed that small complexes and small arrays are intermediates in the formation of large native arrays (Briegel *et al.*, 2014). In the absence of CheA and CheW, chemoreceptors form non-native arrays called “zippers” in which two receptor layers interact with each other at their cytoplasmic tips (where CheA and CheW normally bind) causing membrane invaginations (Zhang *et al.*, 2007). Interestingly, the basic unit in a zipper is

still a trimer-of-dimers; however, when viewed from the top, these trimers-of-dimers exhibit tighter packing than in native arrays (Briegel *et al.*, 2014).

### **Organization of chemoreceptors in other bacteria.**

Chemotaxis in motile prokaryotes depends on tightly coupled chemoreceptor arrays that are responsible for high sensitivity (Duke and Bray, 1999), signal gain (Sourjik and Berg, 2002), cooperativity (Sourjik and Berg, 2004), and adaptation (Li and Hazelbauer, 2005) of the signal transduction system. Given the major role that chemoreceptor arrays play in signal processing, it is not surprising that this organization is likely universal in motile bacteria and Archaea. Cryo-ET studies of 13 distantly related bacteria (Table 1) from 6 distinct taxonomic groups, which together possess chemoreceptors from 7 signaling domain classes confirmed this assumption. All species analyzed in this study possessed chemoreceptors arrays organized as trimers-of-dimers (Briegel *et al.*, 2009).

Most of the trimers-of-chemoreceptor dimers extended in a honeycomb-like lattice with 12 nm spacing (just like in *E. coli*), except for *Listeria monocytogenes* and *Borrelia burgdorferi* where no lattice was visible under the experimental conditions used. The lattice structure was visible the most just above the CheA/CheW baseplate and less ordered near the N-termini of the MCPs, suggesting that the main architectural contacts occur in the signaling subdomain region. A major difference among the species analyzed was in the position of the arrays within a cell. In 6 species (including *E. coli*), the position of the chemoreceptor arrays was polar, while in 2 other species (*Helicobacter hepaticus* and *Campylobacter jejuni*) the arrays completely surrounded the tip of the cell forming a so-called “cap” (Table 1). In *Caulobacter crescentus* and *Vibrio*

*cholerae*, chemoreceptors localized to the convex side of the cell (Briegel *et al.*, 2008; Briegel *et al.*, 2009). The arrays in *Acetonea longum* and *B. burgdorferi* were subpolar and positioned at varying distances from the cell pole (Briegel *et al.*, 2009).

**Table 1. Summary of measurements of 13 different bacterial species obtained by cryo-ET** (modified from Briegel *et al.*, 2009).

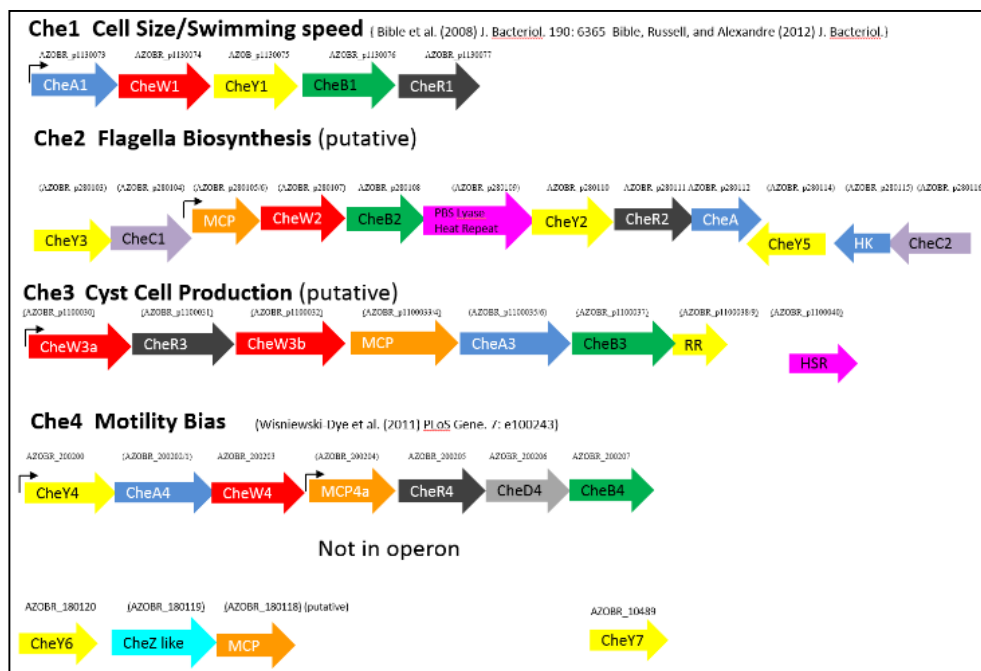
| <b>Bacterium</b>                     | <b>Phylum</b>          | <b>Location of arrays</b>                           |
|--------------------------------------|------------------------|---|
| <i>Thermotoga maritima</i>           | Thermotogae            | Polar   |
| <i>Listeria monocytogenes</i>        | Firmicutes             | Polar   |
| <i>Acetonea longum</i>               | Firmicutes             | Subpolar  |
| <i>Borrelia burgdorferi</i>          | Spirochaetes           | Subpolar  |
| <i>Treponema primitia</i>            | Spirochaetes           | Polar   |
| <i>Caulobacter crescentus</i>        | Alpha- proteobacteria  | Polar,convex side<br>(Briegel <i>et al.</i> , 2008) |
| <i>Magnetospirillum magneticum</i>   | Alpha- proteobacteria  | Polar   |
| <i>Rhodobacter sphaeroides</i>       | Alpha- proteobacteria  | Polar   |
| <i>Escherichia coli</i>              | Gamma-proteobacteria   | Mainly polar<br>(Zhang <i>et al.</i> , 2007)        |
| <i>Vibrio cholerae</i>               | Gamma-proteobacteria   | Polar, convex side                                  |
| <i>Halothiobacillus neapolitanus</i> | Gamma-proteobacteria   | Polar   |
| <i>Helicobacter hepaticus</i>        | Epsilon-proteobacteria | Polar, “cap”  |
| <i>Campylobacter jejuni</i>          | Epsilon-proteobacteria | Polar, “cap”  |

The bacterial species in the cryo-ET study by Briegel *et al.* included chemoreceptors from 7 signaling domain classes (2009). However, each chemoreceptor array visualized by cryo-ET consisted of chemoreceptors belonging to only one major signaling class (44H, 40H, 38H, 36H, and 34H). This conclusion was made based on the fact that the physical length of the signaling domain, defined as the distance between the CheA/CheW baseplate and the inner membrane, correlated with chemoreceptors sequence lengths. For example, chemoreceptor arrays analyzed in *C. jejuni* and *H. hepaticus* were predicted to only include chemoreceptors from the 40H class, even though these species also contained receptors of another class (28H). In these species, the distance between the inner membrane and the baseplate could only accommodate the receptors of the 40H class and not those of the 28H class. The high degree of conservation of chemoreceptor arrays architecture among diverse bacterial species implies that underlying signaling mechanisms are also conserved.

### **Chemotaxis in *Azospirillum brasilense* is controlled by multiple Che pathways.**

Signal transduction during chemotaxis has been studied in various bacterial species: from enteric *E. coli* to aquatic *T. maritima* (Hazelbauer *et al.*, 2008; Perez and Stock, 2007). Even though all known bacteria have chemotaxis proteins similar to those found in *E. coli*, many of them have multiple chemotaxis operons as well as additional chemotaxis proteins and chemoreceptors (Porter *et al.*, 2011). For example, more than 50% of sequenced genomes from chemotactic bacteria contain more than one *cheA* (Porter *et al.*, 2008; Wuichet and Zhulin, 2010). One such species is *Azospirillum brasilense*, a soil alphaproteobacterium that colonizes roots of agronomically important plants (beans, tomatoes, grasses, etc.) and promotes their growth (Dobbelaere and Okon, 2007). The ability of bacteria to become established in the

rhizosphere is strongly correlated with their ability to perform chemotaxis. Indeed, non-chemotactic mutants were impaired in plant root colonization when competing with the wild type *A. brasilense* parental strain (Greer-Phillips *et al.*, 2004).



**Figure 4. *Azospirillum brasilense* has four chemotaxis-like operons.** Chemotaxis genes are also spread in the *A. brasilense* genome in clusters. Most chemotaxis receptors are scattered at various loci on the genome.

The genome of the wild type *A. brasilense* Sp245 and FP2 strains contains 4 chemotaxis operons and 41 chemoreceptors (Figure 4). To date, only one out of the four chemotaxis-like pathways (Che1) has been experimentally characterized (Bible *et al.*, 2008). The Che1 pathway in *A. brasilense* contributes to chemotaxis via an effect on the swimming speed (equivalent to “runs” in *E. coli*) (Bible *et al.*, 2012). Recent evidence suggest that the Che4 pathway is responsible for controlling the swimming reversal frequency (equivalent to tumbles in *E. coli*), and that both Che1 and Che4 contribute to chemotaxis and aerotaxis (Alexandre, 2010; Kumar, 2012; Bible *et al.*, 2012; Russell *et al.*, 2013, unpublished data). Moreover, fluorescent imaging data of CheA1-YFP and CheA4-YFP localization in different mutant backgrounds suggest that components of both Che1 and Che4 operons are required for proper localization of CheA1 and CheA4 to the cell poles: CheA1-YFP and CheA4-YFP fluorescence was diffused in a  $\Delta che1\Delta che4$  strain but not in a  $\Delta che1$  or a  $\Delta che4$  strains (Kumar, 2012).

In addition to multiple Che pathways, the genome of *A. brasilense* encodes 41 chemotaxis receptors, in stark contrast to the 5 chemoreceptors found in the *E. coli* genome (Hazelbauer *et al.*, 2008; Wisniewski-Dye *et al.*, 2011). The sensory specificity of some of the receptors in *A. brasilense* (Tlp1 and AerC) has been determined (transducer like protein 1 (Tlp1) - Greer-Phillips *et al.*, 2004; Russell *et al.*, 2013; AerC (transducer for aerotaxis and related responses, cytoplasmic) – Xie *et al.*, 2010) while sensory specificity of other receptors is yet to be investigated. Even though it is known that certain chemoreceptors in *A. brasilense* interact with more than one Che pathway (Tlp1) and localize to the cell poles (AerC), their exact localization with respect to one another and to other chemotaxis proteins has not been investigated. AerC is a soluble chemoreceptor that localizes to the cell poles under nitrogen-

fixing conditions (absence of nitrogen and low oxygen concentrations) (Xie *et al.*, 2010). Interestingly, its localization to the cell poles is affected in the Che1 deletion background suggesting that it interacts with the chemotaxis proteins in this pathway (Xie *et al.*, 2010). AerC also affects reversal frequency controlled by the signaling output of the Che4 operon, suggesting that this soluble chemoreceptor interacts with proteins in the Che4 pathway (Xie *et al.*, 2010; Kumar, 2012).

Tlp1 is another energy taxis transducer that is important for plant root colonization, redox taxis, and taxis to oxygen and nitrate (Greer-Phillips *et al.*, 2004; Russell *et al.*, 2013). Tlp1 modulates changes in swimming velocity and in reversal frequency via Che1 as well as another unidentified Che pathway, which is hypothesized to be Che4. Thus, Tlp1 may also interact with the chemotaxis proteins in more than one Che pathway (Russell *et al.*, 2013). Together these data suggest that Che1 and Che4 pathways may cross-talk to coordinate chemotaxis behaviors, and that this cross-talk may originate at the level of chemotaxis receptors adding further complexity to the study of chemotaxis in this organism.

This work aims to provide insight into localization of chemoreceptors AerC, Tlp1, and Tlp4a within a cell, in respect to one another and to CheA1 and CheA4 proteins. To date, it is unknown whether chemoreceptors in *A. brasilense* form mixed clusters like in *E. coli*. Whether some receptors preferentially interact with a specific CheA or with both CheA1 and CheA4 is also unknown. We utilized fluorescence microscopy to investigate whether localization of chemoreceptors depends on CheA1 and/or CheA4 proteins and whether their localization depends on one another. We also used Bacteria Two Hybrid Assay to investigate *in vivo*



interactions of chemoreceptors with one another and chemotaxis proteins from Che1 and Che4 pathways.

## **CHAPTER II. Materials and Methods**

### **Strains and growth conditions.**

Cells of the following bacterial strains (*A. brasilense* Table 2) were grown in liquid MMAB (minimal medium for *A. brasilense*) with shaking (200 rpm) at 28°C to OD<sub>600</sub> (optical density at 600 nm) 0.6-1. Liquid MMAB was prepared by adding 3 g K<sub>2</sub>HPO<sub>4</sub>, 1 g NaH<sub>2</sub>PO<sub>4</sub>, 0.15 g KCl, trace amounts of Na<sub>2</sub>MoO<sub>4</sub>, 5 g of malate (carbon source), and 1 g of NH<sub>4</sub>Cl (nitrogen source) to one liter of deionized water and autoclaved for 30 min at 121°C. The following salts were added after autoclaving: 5ml of MgSO<sub>4</sub> (60g/L stock), 500 µl of CaCl<sub>2</sub> (20g/L stock), and 250µl of FeSO<sub>4</sub> (0.631g FeSO<sub>4</sub>.7H<sub>2</sub>O and 0.592g EDTA in 50ml water). To induce nitrogen fixation, cells grown in MMAB (with carbon and nitrogen) were pelleted and washed 3 times with MMAB without nitrogen, and subsequently incubated in MMAB (supplemented with carbon but not nitrogen) at 28°C without shaking to ensure low aeration for 6 hours-overnight. All culture stocks were routinely maintained on solid MMAB medium (liquid MMAB supplemented with 15 g/L agar) lacking nitrogen source.

**Table 2. Plasmids and strains used in this study.**

| Strains/plasmids                        | Genotype, relevant characteristics   | Reference/source                       |
|---|--|--|
| <i>A. brasilense</i> strains            |  |  |
| Sp7 (wt)                                | Wild type strain   | ATCC 29145                             |
| $\Delta cheA1$                          | $\Delta(cheA1)$ , Km   | Bible <i>et al.</i> , 2008             |
| $\Delta cheA4$                          | $\Delta(cheA4)$ , Gm   | Alexandre lab, unpublished             |
| $\Delta cheA1 \Delta cheA4$             | $\Delta(cheA1) \Delta(cheA4)$ , Km Gm  | Alexandre lab, unpublished             |
| $\Delta aerC$                           | $\Delta(aerC)$ , Km  | Xie <i>et al.</i> , 2010               |
| $\Delta tlp1$                           | $\Delta(tlp1)$ , Km  | Greer-Phillips <i>et al.</i> , 2004    |
| wt (pRH_Tlp1)                           | <i>A. brasilense</i> Sp7 expressing a Tlp1-YFP fusion from the pRH005 plasmid; Km Cm   | Alexandre lab, unpublished             |
| $\Delta cheA1$ (pRH_Tlp1)               | <i>A. brasilense</i> Sp7 mutant derivative deleted for <i>cheA1</i> and expressing a Tlp1-YFP fusion from the pRH005 plasmid; Km Cm        | Alexandre lab, unpublished (this work) |
| $\Delta cheA4$ (pRH_Tlp1)               | <i>A. brasilense</i> Sp7 mutant derivative deleted for <i>cheA4</i> and expressing a Tlp1-YFP fusion from the pRH005 plasmid; Km Cm        | Alexandre lab, unpublished (this work) |
| $\Delta cheA1 \Delta cheA4$ (pRH_Tlp1)  | <i>A. brasilense</i> Sp7 mutant derivative deleted for <i>cheA1 cheA4</i> and expressing a Tlp1-YFP fusion from the pRH005 plasmid; Km Cm  | Alexandre lab, unpublished (this work) |
| $\Delta tlp1$ (pRH_Tlp1)                | <i>A. brasilense</i> Sp7 mutant derivative deleted for <i>tlp1</i> and expressing a Tlp1-YFP fusion from the pRH005 plasmid; Km Cm         | Russell <i>et al.</i> , 2013           |
| $\Delta aerC$ (pRH_Tlp1)                | <i>A. brasilense</i> Sp7 mutant derivative deleted for <i>aerC</i> and expressing a Tlp1-YFP fusion from the pRH005 plasmid; Km Cm         | Alexandre lab, unpublished (this work) |
| wt (pRH_Tlp4a)                          | <i>A. brasilense</i> Sp7 expressing a Tlp4a-YFP fusion from the pRH005 plasmid; Km Cm  | Alexandre lab, unpublished             |
| $\Delta cheA1$ (pRH_Tlp4a)              | <i>A. brasilense</i> Sp7 mutant derivative deleted for <i>cheA1</i> and expressing a Tlp4a-YFP fusion from the pRH005 plasmid; Km Cm       | Alexandre lab, unpublished (this work) |
| $\Delta cheA4$ (pRH_Tlp4a)              | <i>A. brasilense</i> Sp7 mutant derivative deleted for <i>cheA4</i> and expressing a Tlp4a-YFP fusion from the pRH005 plasmid; Km Cm       | Alexandre lab, unpublished (this work) |
| $\Delta cheA1 \Delta cheA4$ (pRH_Tlp4a) | <i>A. brasilense</i> Sp7 mutant derivative deleted for <i>cheA1 cheA4</i> and expressing a Tlp4a-YFP fusion from the pRH005 plasmid; Km Cm | Alexandre lab, unpublished (this work) |
| $\Delta tlp1$ (pRH_Tlp4a)               | <i>A. brasilense</i> Sp7 mutant derivative deleted for <i>tlp1</i> and expressing a Tlp4a-YFP fusion from the pRH005 plasmid; Km Cm        | Alexandre lab, unpublished             |
| $\Delta aerC$ (pRH_Tlp4a)               | <i>A. brasilense</i> Sp7 mutant derivative deleted for <i>aerC</i> and expressing a Tlp4a-YFP fusion from the pRH005 plasmid; Km Cm        | Alexandre lab, unpublished (this work) |
| $\Delta aerC$ (pRH_Tlp2)                | <i>A. brasilense</i> Sp7 mutant derivative deleted for <i>aerC</i> and expressing a Tlp2-YFP fusion from the pRH005 plasmid; Km Cm         | Alexandre lab, unpublished (this work) |

**Table 2 (continued)**

| Strains/plasmids                | Genotype, relevant characteristics   | Reference/source              |
|---------------------------------|--|-------------------------------|
| <i>E. coli</i> strains/plasmids |  |                               |
| TOPO 2.1                        | PCR cloning vector, Km   | Invitrogen                    |
| pRH005                          | Gateway-based destination vector expressing proteins fused with YFP at their C-terminus; Km Cm                   | Hallez <i>et al.</i> , 2007   |
| pRH_AerC                        | pRH005 containing an <i>aerC</i> promoter region and ORF; Km Cm  | Xie <i>et al.</i> , 2010      |
| pRH_Tlp1                        | pRH005 containing a <i>tlp1</i> promoter region and ORF; Km Cm   | Russell <i>et al.</i> , 2013  |
| pRH_Tlp4a                       | pRH005 containing a <i>tlp4a</i> promoter region and ORF; Km Cm  | Alexandre lab, unpublished    |
| pRH_Tlp2                        | pRH005 containing a <i>tlp2</i> promoter region and ORF; Km Cm   | Russell <i>et al.</i> , 2013  |
| pUT18                           | Derivative of pUC19 plasmid encoding T18 of CyA, Cb  | Karimova <i>et al.</i> , 1998 |
| pKNT25                          | Derivative of pSU40 plasmid encoding T25 of CyA, Km  | Karimova <i>et al.</i> , 1998 |
| pUT18C-zip                      | a derivative of pUT18C in which the leucine zipper of GCN4 is genetically fused in frame to the T18 fragment, Cb | Karimova <i>et al.</i> , 1998 |
| pKT25-zip                       | a derivative of pKT25 in which the leucine zipper of GCN4 is genetically fused in frame to the T25 fragment, Km  | Karimova <i>et al.</i> , 1998 |
| pUT18_cheA4                     | pUT18 containing <i>cheA4</i> , Cb   | Alexandre lab, unpublished    |
| pUT18_cheW4                     | pUT18 containing <i>cheW4</i> , Cb   | Alexandre lab, unpublished    |
| pUT18_tlp1                      | pUT18 containing <i>tlp1</i> , Cb  | Alexandre lab, unpublished    |
| pUT18_aerC                      | pUT18 containing <i>aerC</i> , Cb  | Alexandre lab, unpublished    |
| pUT18_tlp4a                     | pUT18 containing <i>tlp4a</i> , Cb   | Alexandre lab, unpublished    |
| pUT18_cheA1                     | pUT18 containing <i>cheA1</i> , Cb   | Alexandre lab, unpublished    |
| pUT18_cheW1                     | pUT18 containing <i>cheW1</i> , Cb   | Alexandre lab, unpublished    |
| pKNT25_cheA4                    | pKNT25 containing <i>cheA4</i> , Km  | Alexandre lab, unpublished    |
| pKNT25_cheW4                    | pKNT25 containing <i>cheW4</i> , Km  | Alexandre lab, unpublished    |
| pKNT25_tlp1                     | pKNT25 containing <i>tlp1</i> , Km   | Alexandre lab, unpublished    |
| pKNT25_aerC                     | pKNT25 containing <i>aerC</i> , Km   | Alexandre lab, unpublished    |
| pKNT25_tlp4a                    | pKNT25 containing <i>tlp4a</i> , Km  | Alexandre lab, unpublished    |
| pKNT25_cheA1                    | pKNT25 containing <i>cheA1</i> , Km  | Alexandre lab, unpublished    |
| pKNT25_cheW1                    | pKNT25 containing <i>cheW1</i> , Km  | Alexandre lab, unpublished    |
| pKNT25_aerC                     | pKNT25 containing <i>aerC</i> , Km   | Alexandre lab, unpublished    |
| S17.1                           | <i>thi endA recA hsdR</i> with RP4-2Tc::Mu-Km::Tn7 integrated in chromosome                                      | Simon <i>et al.</i> , 1983    |

**Table 2 (continued)**

| Strains/plasmids | Genotype, relevant characteristics  | Reference/source              |
|------------------|---|-------------------------------|
| Top10            | General cloning strain  | Invitrogen                    |
| BTH101           | F <sup>-</sup> <i>cya-99 araD139 galE15 galK16 rpsL1 hsdR2 mcrA1 mcrB1</i>                                      | Karimova <i>et al.</i> , 1998 |
| XL-1 Blue        | <i>recA1 endA1 gyrA96 thi-1 hsdR17 supE44 relA1 lac</i> [F' <i>proAB lacIq</i> ZΔM15 Tn10 (Tet <sup>r</sup> )]. | Agilent Technologies          |

Antibiotics used : Km – kanamycin (50 µg/mL or 30 µg/mL), Cm- chloramphenicol (34 µg/mL), Gm – gentamycin (20 µg/mL), Cb – carbenicillin (50 µg/mL), Tet – tetracyclin (10 µg/mL).

#### **Plasmids/strains construction and fluorescence microscopy.**

Fluorescently tagged YFP constructs were previously made in the lab by Gateway cloning (Xie *et al.*, 2010; Bible, 2012; Kumar, 2012) and were introduced into Sp7 and other strains (Table 2) by biparental mating as described in Hauwaerts *et al.*, 2002. One mL of cells grown as described above were pelleted at 5,000 rpm for 2 min. Twenty µL of the pelleted cells were mounted on the microscope glass slide containing a 100 µL agarose pad (1% LMP agarose in 1xPBS buffer – NaCl 8g/L, KCl 0.2 g/L, KH<sub>2</sub>PO<sub>4</sub> 0.24 g/L, Na<sub>2</sub>HPO<sub>4</sub> 0.144 g/L, pH 7) and covered with a cover slip. The cells were visualized using a Nikon ECLIPSE 80i fluorescence microscope equipped with a Nikon CoolSnap HQ2 cooled CCD camera, after 2-3 hours or after being on a slide overnight. The YFP HYQ filter from Nikon was used (Excitation 490-510 nm,

Emission – 520-550 nm, Mirror – 515, exposure – 5s, calibrated gain – 4x) for collecting the images.

The images were quantified using the Nikon NIS-Elements BR program (Nikon) by calculating the ratio of average fluorescence intensity in the polar foci compared to the cell body. The cell lengths and the distances from the pole to the fluorescent foci were measured using straight line tool in ImageJ software (<http://imagej.nih.gov/ij/>). At least 80 cells from 5 different fields of view (3 independent experiments) were analyzed for each strain. The results were graphed and analyzed statistically using GraphPad Prism software (<http://www.graphpad.com/prism/prism.htm>) and MS Excel 2013. All graphs display the mean and standard deviation.

### **Evaluating protein expression using Western blotting.**

Bacterial cells grown in MMAB minimal medium supplemented with carbon and nitrogen source were harvested and washed once with 1XPBS and resuspended in 0.2 mL of RIPA buffer (50 mM Tris-HCl, 150 mM NaCl, 1% Triton X-100, 0.1% SDS, pH 8.0 ).The cells were disrupted by sonication. Cell debris were removed by centrifugation at  $20,800 \times g$  for 10 min at 4 °C. Protein concentrations were determined by the Bradford method (Pierce) according to the manufacturer's instructions. A cell lysate (10 µg of protein) was run in a 12% SDS-polyacrylamide gel, and transferred onto a 45 µm nitrocellulose membrane (Bio-Rad). Immunoblots were carried out with an anti-GFP antibody (which crossreacts with YFP, a gift from R. Goodchild) at a 1:1,000 dilution in 1% nonfat dry milk in 1XTTBS (3.03 g/500 mL Tris, 4.38 g/500 mL NaCl, pH 7.5). The membrane was incubated overnight at room temperature,

washed three times with 1XTTBS, and incubated with the HRP-conjugated goat anti-rabbit antibody at a 1:5,000 dilution for 1 hour at room temperature (ImmunoReagents, Inc.). After being washed three times in 1XTTBS, the membrane was incubated with Luminata Forte Western HRP Substrate (Millipore) for 2 min and exposed to X-ray film (exposure to film 30 seconds – 1 minute).

### **Bacteria-Two Hybrid Assay (BACTH).**

BACTH was used to investigate protein-protein interactions. Proteins of interest (CheA1, CheA4, CheW1, CheW4, Tlp1, AerC, and Tlp4a) were fused on the C-termini to the T18 and T25 domains of *Bordetella pertussis* adenylate cyclase present in vectors pUT18 and pKNT25, respectively, essentially as described by the manufacturer's protocol (Euromedex). The genes of interest were first PCR-amplified (

Table 3) and cloned into TOPO 2.1 vector (Invitrogen). The resulting vectors were digested with the following enzyme pairs (HindIII and EcoRI for *cheA4*, *cheW1*, *cheW4*, *tlp1*, and *tlp4a*; HindIII and KpnI for *cheA1* and *aerC*) and ligated into their destination vectors (pUT18 and pKNT25) that were previously digested with the same enzymes using T4 ligation (New England Bio Labs). Resulting plasmids were propagated in XL-1 Blue cells (Agilent Technologies), and the presence of the inserts was confirmed by colony PCR using the following settings (

Table 4). To test for interactions, two plasmids expressing genes of interest were co-transformed into BTH101 competent cells and plated on LB plates (10 g Tryptone, 5 g Yeast Extract, 10 g NaCl, 15% agar) with kanamycin (50 µg/mL) and carbenicillin (50 µg/mL). The plates were incubated for 2 days at 30°C. Two microliters of overnight LB liquid cultures (4-5

colonies/5 mL LB with kanamycin (50 µg/mL) and carbenicillin (50 µg/mL)) grown with shaking (200 rpm) at 30°C) were plated onto MacConkey/lactose (Difco™ ref.212123 MacConkey Agar) plates with kanamycin (50 µg/mL) and carbenicillin (50 µg/mL) and incubated at 30°C for up to 4 days. Empty vectors (pUT18 and pKNT25) were used as negative controls while pUT18-zip and pKT25-zip (Karimova *et al.*, 1998) were used as positive controls. The interaction was considered positive if the colonies turned red above the negative control levels.

**Table 3. Primers.**

| Primer name                    | Sequence                                      |
|--------------------------------|---|
| <b>CheA4 HindIII For BACTH</b> | 5'-AAG CTT ATG GAC GGG GTG CGC AAC AC-3'      |
| <b>CheA4 EcoRI Rev BACTH</b>   | 5' - GAA TTC GAC CGG TTC GAG TGC GGG GGC - 3' |
| <b>Tlp4a HindIII For BACTH</b> | 5' - AAG CTT ATG GCG AAA GGG GTC GGT TCG - 3' |
| <b>Tlp4a EcoRI Rev BACTH</b>   | 5' - GAA TTC TGC CGC CCG TCC GCG GGC CAG - 3' |
| <b>CheW4 HindIII For BACTH</b> | 5' - AAG CTT ATG AGC AGT TCCACCGCGCTC-3'      |
| <b>CheW4 EcoRI Rev BACTH</b>   | 5' - GAA TTC GGA TGC CCG CTC CAG CGC CGG - 3' |
| <b>Tlp1 HindIII For BACTH</b>  | 5' - AAG CTT ATG AAT CCC CTC CGC ACG TTC - 3' |
| <b>Tlp1 EcoRI Rev BACTH</b>    | 5' - GAA TTC GGC GAC CGC CGG AAG CGG GTG -3'  |
| <b>AerC HindIII For BACTH</b>  | 5- AAG CTT ATG CCC TTT AAA ACC TTT CTA - 3'   |
| <b>AerC KpnI Rev BACTH</b>     | 5'-GGT ACC ACG GGC CAG CAC CTT GGC GGC-3      |
| <b>CheW1 HindIII For BACTH</b> | 5' - GC AAG CTTG ATG AGC AAC GCC AAG CTG- 3'  |
| <b>CheW1 EcoRI Rev BACTH</b>   | 5' - GC GAA TTCG GGC CGC TTC CAT CGT GGT - 3' |
| <b>CheA1ΔTM HindIII For</b>    | 5' - GC AAG CTTA GAC CGC CTG CCC TAC AAC- 3'  |
| <b>CheA1ΔTM KpnI Rev BACTH</b> | 5'-GC GGT ACC TGC GGC ACC TTT CTG CTC -3'     |



**Table 4. Colony PCR conditions.**

| <b>Step</b>          | <b>Temperature</b>                | <b>Time</b>    |
|----------------------|-----------------------------------|----------------|
| Initial Denaturation | 95°C                              | 2 minutes      |
| 30 Cycles            | 95°C                              | 1 minute       |
|                      | Average T <sub>m</sub> of primers | 45 seconds     |
|                      | 72°C                              | 1.30 minute/kb |
| Final Extension      | 72°C                              | 5 minutes      |
| Hold                 | 4-10°C                            |                |

## CHAPTER III. Results

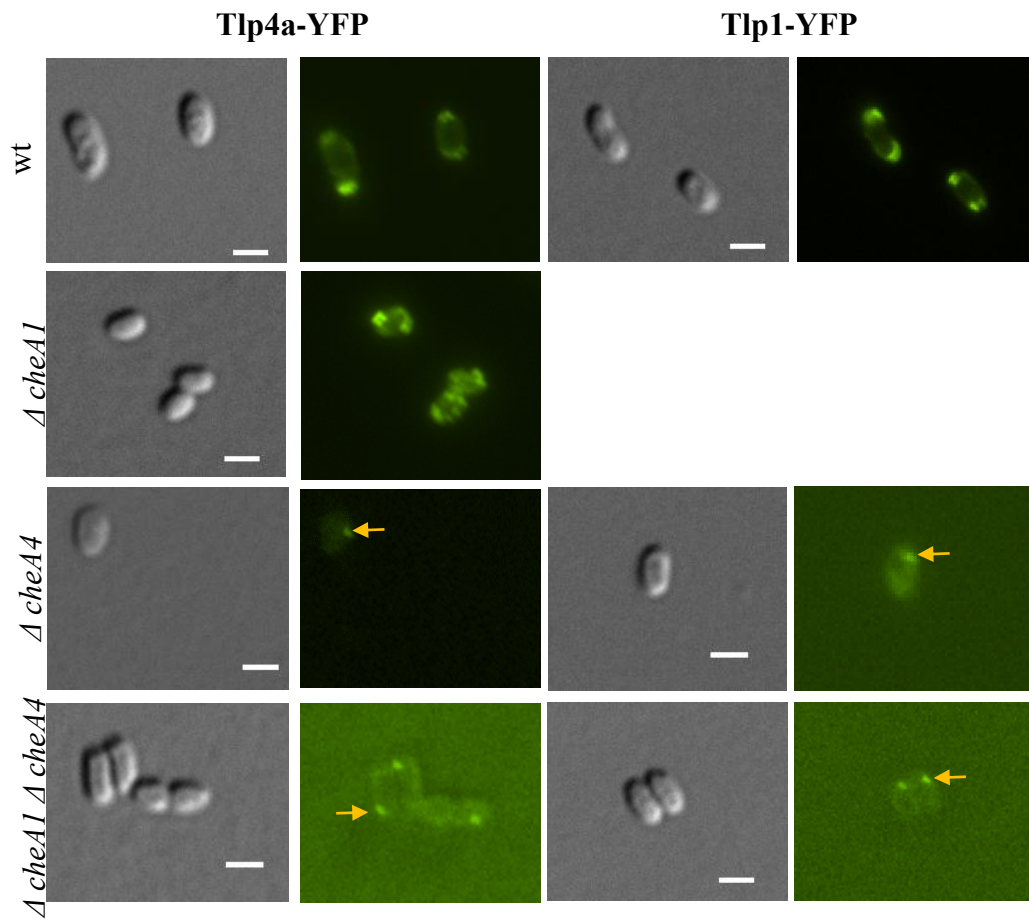
In a model organism *E. coli*, chemoreceptors form mixed clusters and subsequently large arrays that localize to the cell poles along with the CheA histidine kinase and the CheW coupling protein as revealed by PALM (photoactivated localization microscopy), fluorescence microscopy, and cross-linking studies (Greenfield *et al.*, 2009; Kentner, 2006; Studdert and Parkinson, 2003). Cryo-ET studies of 13 distinct bacterial species showed that such architecture is universally conserved and likely contributes to signal gain and amplification (Briegel *et al.*, 2009). Interaction of chemoreceptors with the histidine kinase CheA is required for chemotaxis signaling but it appears not to be required for chemoreceptor cluster formation (Kentner *et al.*, 2006). Since more than half of the bacterial species, which genomes have been sequenced, contain more than one CheA homologue, it is unknown how multiple CheAs and numerous receptors affect formation of chemoreceptors clusters. The genome of the alphaproteobacterium *A. brasilense* encodes for 41 chemoreceptors, and several CheA and CheW homologs (Wisniewsky-Dye *et al.*, 2012). In this work we determined whether chemoreceptors require the presence of CheA1 and/or CheA4 as well as other chemoreceptors to localize at the cell poles using fluorescent microscopy. We also used BACTH assay to determine *in vivo* interactions of chemoreceptors with one another and chemotaxis proteins from Che1 and Che4 pathways.

### **CheA4 is required for polar localization of Tlp4a-YFP and Tlp1-YFP fluorescent foci.**

When YFP fusion proteins were expressed in the wild type background (Sp7) both Tlp1-YFP and Tlp4a-YFP localized at either one or both cell poles as tight fluorescent foci (Figure 5). In the absence of CheA1 ( $\Delta$ *cheA1* strain), the Tlp4a-YFP exhibited a different distribution

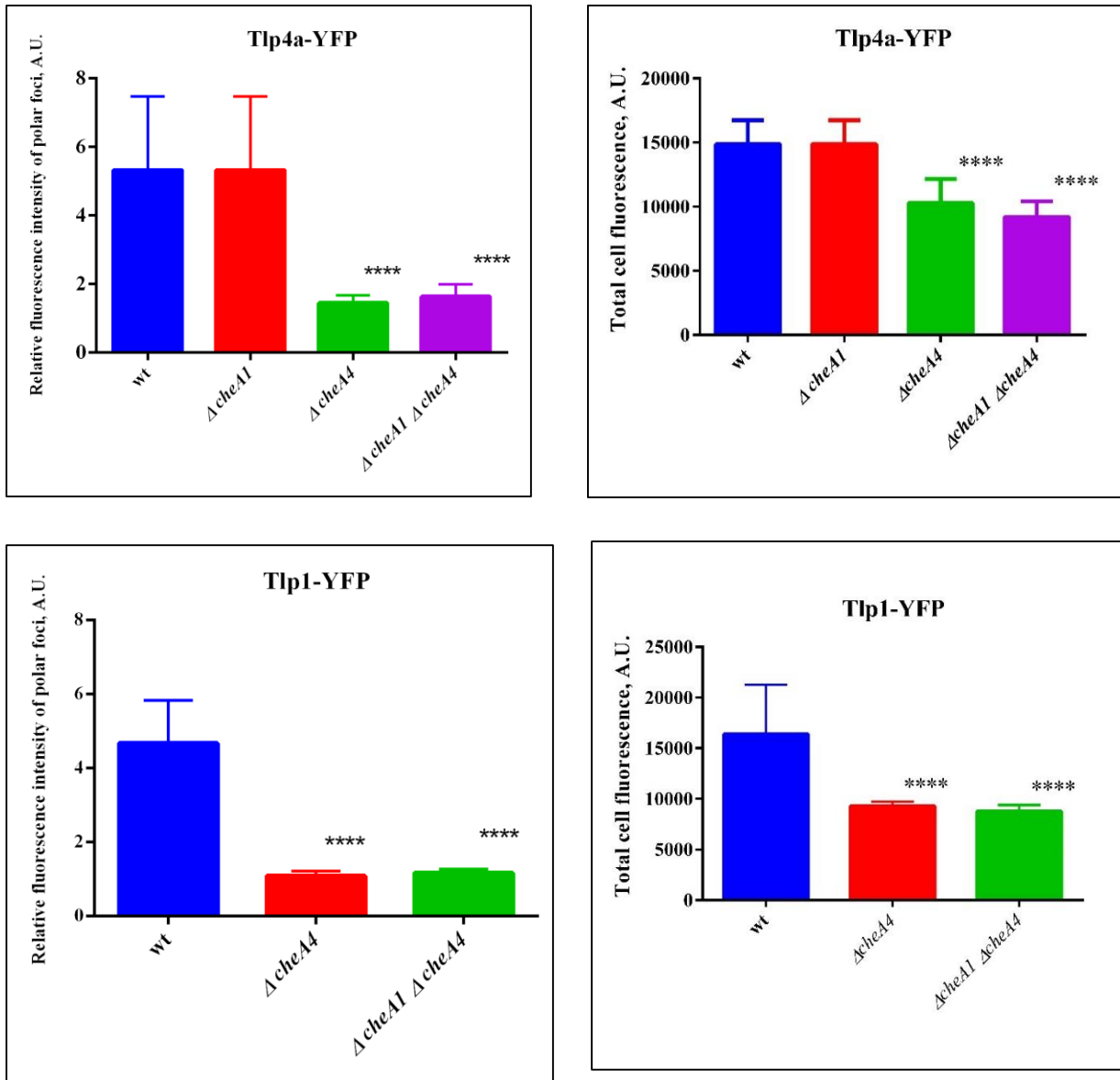
compared to the wild type: more lateral fluorescent foci along with the polar ones that looked like the wild-type clusters. The average number of foci per cell in the wild type background was  $2.1 \pm 0.7$  while the number of foci per cell in the  $\Delta cheA1$  strain was significantly different from that and equaled to  $3.8 \pm 1.3$  (p-value < 0.0001, N=90). Despite the change in distribution of Tlp4a-YFP fluorescence within the cells, the relative fluorescence intensity of the polar clusters in the  $\Delta cheA1$  strain was not significantly different from the wild-type (Figure 6, p-value > 0.05). In the absence of CheA4 ( $\Delta cheA4$  strain) and both CheA1 and CheA4 proteins ( $\Delta cheA1 \Delta cheA4$  strain), Tlp4a-YFP and Tlp1-YFP clusters appeared more diffused and dimmer than in the wild type strain (Figure 5 and Figure 6). In addition, roughly 50% of cells expressing Tlp1-YFP in the  $\Delta cheA4$  background lacked any visible fluorescent focus and rather, exhibited diffuse fluorescence throughout the cytoplasm (data not shown). The relative fluorescence intensity of the Tlp4a-YFP and Tlp1-YFP polar foci was also significantly lower in both the  $\Delta cheA4$  and the  $\Delta cheA1 \Delta cheA4$  backgrounds, compared to the wild type strain (Figure 6, p-value < 0.0001). In addition to being dimmer, both Tlp4a-YFP and Tlp1-YFP clusters were mislocalized, locating slightly on the side of the cell pole, in contrast to the consistent polar subcellular organization of fluorescent clusters in the wild type strain (Figure 7). Figure 7 illustrates this observation in quantitative terms : the majority of cells expressing Tlp4a-YFP and Tlp1-YFP in the wild type background contained polar fluorescent foci, while in the  $\Delta cheA4$  and  $\Delta cheA1 \Delta cheA4$  backgrounds, the majority of cells displayed mislocalized foci (Figure 7B). In addition, measuring the distances of the fluorescent clusters from the cell poles (Figure 7A) demonstrated that the majority of Tlp4a-YFP and Tlp1-YFP clusters were polar in the wild type background, while localization of Tlp4a-YFP and Tlp1-YFP clusters was aberrant in both the  $\Delta cheA4$  and

*ΔcheA1 ΔcheA4* strains with the majority of the fluorescent clusters located between cell poles, i.e. on the side of the cells. Altogether, these data suggest that CheA4 is required for localization of Tlp1-YFP and Tlp4a-YFP at the cell pole and proper cluster formation.



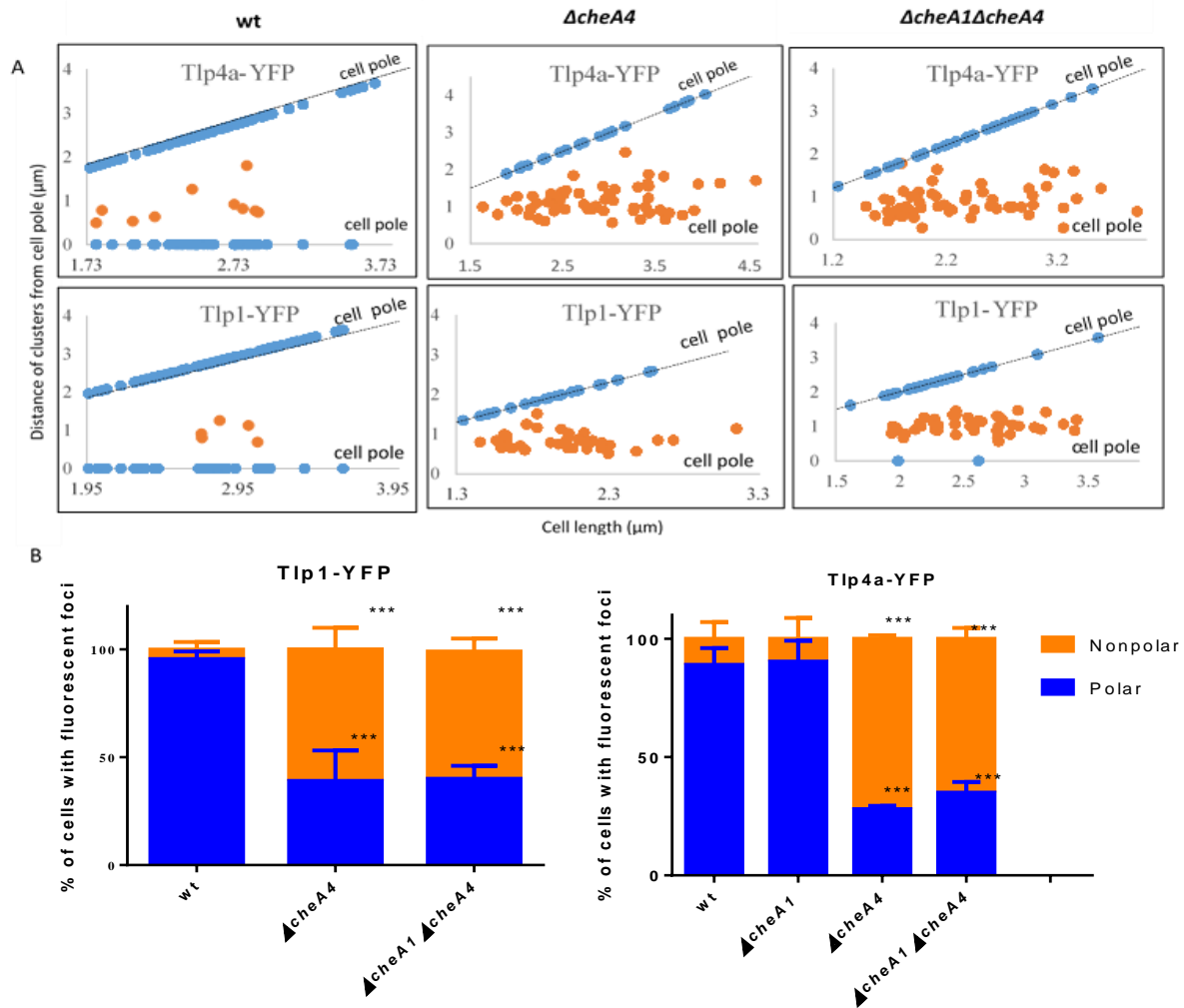
**Figure 5. CheA4 is required for proper localization of chemoreceptors.**

Fluorescent microscopy images of Tlp1-YFP and Tlp4a-YFP in the wild type and mutant backgrounds. The cells were grown to similar  $OD_{600}$  and immobilized on 1% agarose pad in 1XPBS. Images were acquired after 2-3 hours on the pad (wt,  $\Delta cheA1$ ) or after 16-24 hrs ( $\Delta cheA4$  and  $\Delta cheA1 \Delta cheA4$ ). Orange arrows point at non-polar (mislocalized) foci, scale bars – 2  $\mu$ m.



**Figure 6. Relative fluorescence intensity and total cell fluorescence of Tlp1-YFP and Tlp4a-YFP is decreased in  $\Delta cheA4$  and  $\Delta cheA1 \Delta cheA4$  backgrounds compared to the wild type.** Bar graphs depict fluorescence intensity of the polar foci relative to the fluorescence intensity of the cell body and total cell fluorescence (fluorescence of the polar foci plus fluorescence of the cell body). All data are shown as mean +1SD.  $N \geq 80$  cells.

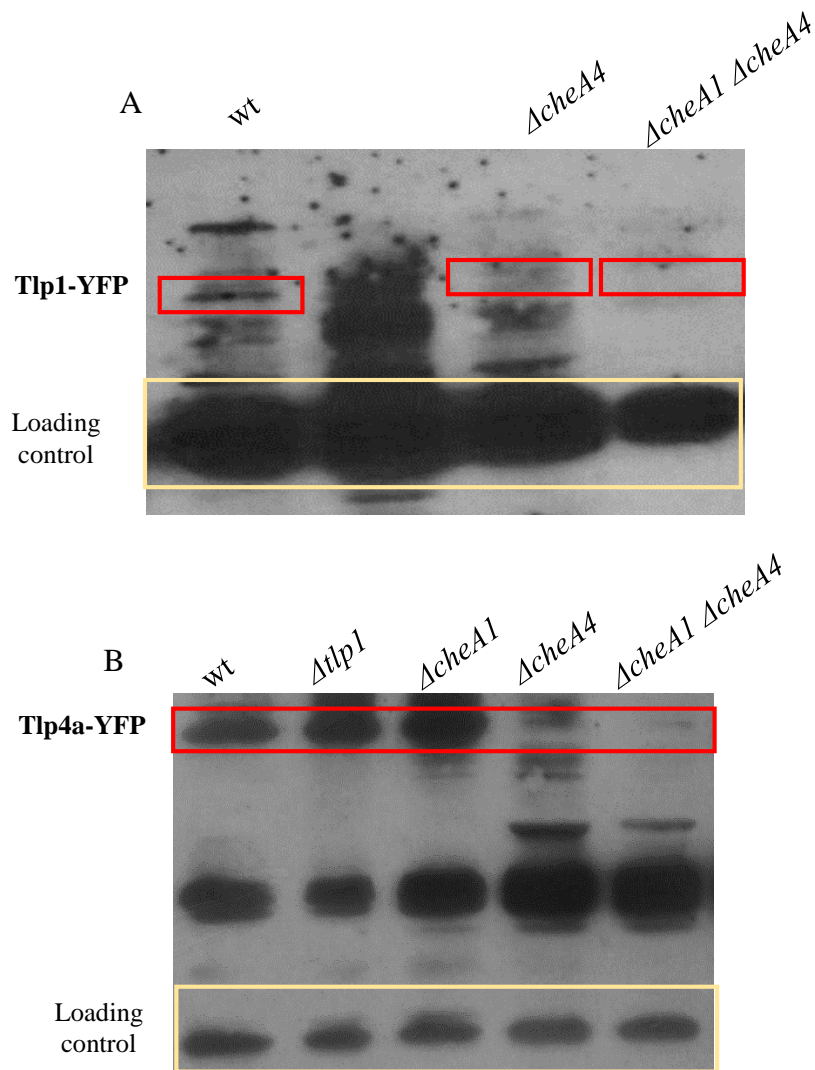
\*\*\*\*- p-value<0.0001



**Figure 7. Tlp1-YFP and Tlp4a-YFP fluorescent foci appear mislocalized in the  $\Delta cheA4$  and  $\Delta cheA1 \Delta cheA4$  backgrounds.** (A) Graphs depict the distance of Tlp1-YFP and Tlp4a-YFP clusters from the cell poles as a function of cell length (blue dots represent fluorescent foci at the pole, orange dots represent mislocalized foci). (B) Stacked bar graphs depict polar (blue) and nonpolar (orange) localization of Tlp1-YFP and Tlp4a-YFP clusters. All data are shown as mean +1SD, \*\*\* - p-value<0.001,  $N \geq 80$  cells.

Another consistent observation was made during imaging: fluorescent foci of Tlp4a-YFP and Tlp1-YFP were visible after cells were immobilized on the agarose pad 2-3 hours, in the wild type and  $\Delta cheA1$  backgrounds (Tlp4a-YFP); however, under the same conditions, Tlp1-YFP and Tlp4a-YFP fluorescence was initially diffused in the  $\Delta cheA4$  and not visible in the  $\Delta cheA1 \Delta cheA4$  background. It took at least 16-24 hours after the cells were placed on the agarose pad to be able to image fluorescent foci in the  $\Delta cheA4$  and  $\Delta cheA1 \Delta cheA4$  backgrounds (Figure 5). This observation suggests that formation of visible fluorescent chemoreceptor clusters is slower in  $\Delta cheA4$  and  $\Delta cheA1 \Delta cheA4$  backgrounds than it is in the wild type or  $\Delta cheA1$  strains. This could be caused either by a delayed assembly of chemoreceptor clusters and subsequently arrays or result from a reduced amount of folded proteins: proteins that do not get recruited into the clusters, eventually get degraded. This hypothesis is consistent with the overall decrease in total cell fluorescence intensity observed for Tlp1-YFP and Tlp4a-YFP in  $\Delta cheA4$  and  $\Delta cheA1 \Delta cheA4$  strains (Figure 6).





**Figure 8. Cellular levels of Tlp1-YFP and Tlp4a-YFP expressed from pRH005 plasmid.**

Equivalent total protein concentrations were analyzed in all samples. Expression of Tlp1-YFP and Tlp4a-YFP from pRH005 plasmid was probed with anti-GFP primary antibody (1:1,000 dilution). Bands in red boxes are the bands corresponding to Tlp1-YFP (panel A) and Tlp4a-YFP (panel B). The bands in yellow boxes represent loading controls. Tlp1-YFP and Tlp4a-YFP get degraded in  $\Delta cheA4$  and  $\Delta cheA1 \Delta cheA4$  strains.

To evaluate protein expression and address these questions, we performed Western blotting experiments on fluorescently tagged proteins (Tlp1-YFP and Tlp4a-YFP) in the wild type and mutant strains. When probed with anti-GFP antibody, Tlp1-YFP expressed from pRH005 plasmid was degraded in  $\Delta cheA4$  strain (no band present) and  $\Delta cheA1 \Delta cheA4$  strain while the band in the wild type strain was sharp indicating normal expression (Figure 8). When Tlp4a-YFP expression was evaluated in the wild type and mutant strains, we found that it was degraded in the  $\Delta cheA4$  (faint band present) and  $\Delta cheA1 \Delta cheA4$  (very faint band present) strains (Figure 8B). In contrast, Tlp4a-YFP expression remains the same in the  $\Delta tlp1$  and  $\Delta cheA1$  strains compared to the wild type strains. These data suggest that reduced fluorescence intensity (both relative and total cell fluorescence) of Tlp1-YFP and Tlp4a-YFP in the  $\Delta cheA4$  and  $\Delta cheA1 \Delta cheA4$  strains is due to protein degradation. It is possible that these proteins do not get recruited to the clusters are degraded.

#### ***In vivo* interactions of chemoreceptors with chemotaxis proteins in Che1 and Che4 pathways evaluated by Bacteria-Two Hybrid Assay.**





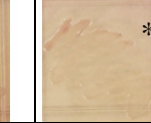
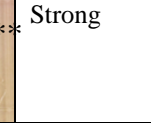
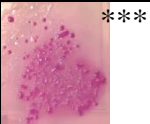
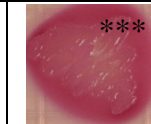
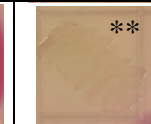
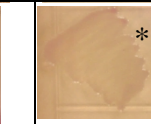
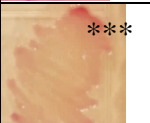



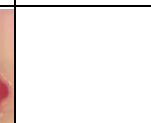





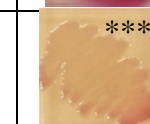
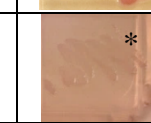
Based on the results of the fluorescence microscopy imaging studies described above, localization of Tlp1 and Tlp4a chemoreceptors is dependent on CheA4. Also, it has been found that Tlp1 signals in a Che1-dependent manner (Russell *et al.*, 2013). In order to evaluate whether chemoreceptors can physically interact with CheA1 and CheA4 as well as coupling proteins CheW1 and CheW4, we utilized a Bacteria-Two Hybrid Assay (BACTH) optimized for analyzing membrane proteins interactions. This assay is based on the reconstitution of two domains (T18 and T25) of adenylate cyclase enzyme from *Bordetella pertussis* (Ladant and Ullmann, 1999). Plasmids expressing fusion proteins were co-transformed into competent cells

(adenylate cyclase deficient *E. coli*), and interactions were determined on MacConkey Agar plates. If protein-protein interactions occur, adenylate cyclase enzyme produces cAMP which in turn activates expression of *lac* operon. As a result, *E. coli* are able to utilize lactose as a carbon source. This can be detected by color change on MacConkey Agar plates: phenol red dye present in MacConkey medium changes color if pH decreases as a result of lactose fermentation (Karimova *et al.*, 1998). Thus, lactose fermenting bacteria appear pink to bright red while bacteria that cannot ferment lactose remain white to very pale pink.

Two types of plasmids expressing fusion proteins (proteins of interest were fused to T18 and T25 domains of *B. pertussis* adenylate cyclase at their C-termini) were used in this experiment: pUT18 – high copy plasmid and pKNT25 – low copy plasmid. Protein-protein interactions were determined using both plasmid combinations. Two vectors pUT18 and pKNT25 that did not contain any inserts were utilized as a negative control while vectors pUT18zip and pKT25zip expressing two parts of a leucine zipper GCN4 were used as a positive control. After incubation on MacConkey Agar plates supplemented with lactose, negative control (cells containing pUT18 and pKNT25) remained white, while the positive control (cells containing pUT18zip and pKT25zip) turned bright red indicating reconstitution of adenylate cyclase enzyme and activation of *lac* operon expression.

To ensure that the assay is suitable for assessing the interactions among *A. brasilense* chemotaxis proteins, we first determined whether CheA4 and CheW4 interact since they were previously found to be interacting using another assay (unpublished data). In addition, CheW4 is a coupling protein encoded within *che4* operon and is, therefore, predicted to be interacting with CheA4. When expressed from both pUT18 and pKNT25 CheA4 and CheW4 exhibited strong

interaction as evidenced by red colonies on MacConkey/lactose (1B and 2A, Figure 9). When expressed from a high copy plasmid, CheA4 strongly interacted with Tlp1 (1C) and showed a weaker interaction with itself (1A), that may be explained by the fact that all CheA proteins form dimers (Figure 9, column 1). A strong positive interaction of CheA4 with Tlp1 when both proteins are expressed from high and low copy vectors (1C and 3A) indicates that CheA4 and Tlp1 interact *in vivo* (Figure 10). In addition, Tlp1 strongly interacted with CheW4 which suggest that Tlp1 may signal through Che4 pathway as previously suggested (Stephens *et al.*, 2006; Russell *et al.*, 2013). Interestingly, Tlp1 did not display a positive interaction with CheW1 or CheA1 (3F and G). CheA1 displayed a strong positive interaction with CheW1, a coupling protein encoded within *che1* operon (as expected), and it also showed strong positive interaction with CheA4 suggesting that CheA1 and CheA4 may form heterodimers (6G and 6A).

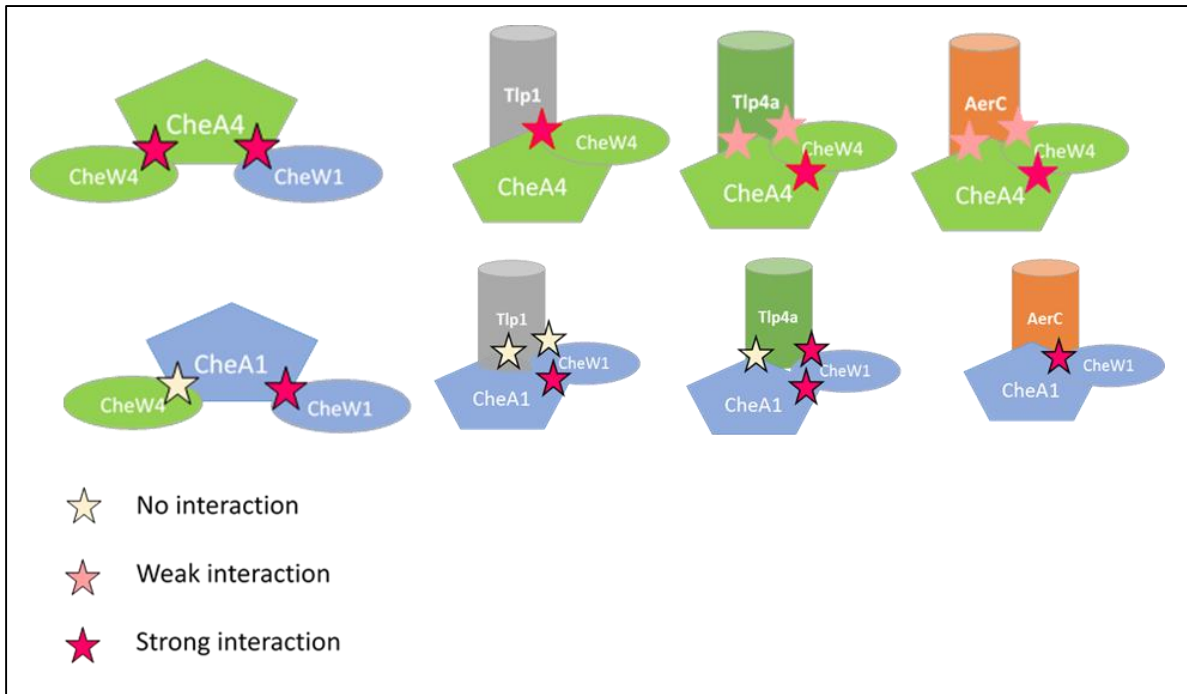
|                   |       | 1   | 2  | 3   | 4  | 5   | 6   | 7  |
|-------------------|-------|---|--|---|--|---|---|--|
| pUT18 (high copy) |       | CheA4   | CheW4  | Tlp1  | Tlp4a  | AerC  | CheA1   | CheW1  |
| pKNT25 (low copy) |       |   |  |   |  |   |   |  |
| A                 | CheA4 |  **  |  *** |  *** |  ** |  **  | Strong  |  ***  |
| B                 | CheW4 |  *** | n/d  |  *** |  ** |  **  | n/d   | No interaction detected  |
| C                 | Tlp1  |  *** | n/d  |  *** | No interaction detected  | n/d   | n/d   | No interaction detected  |
| D                 | Tlp4a |  **  | n/d  | No interaction detected   | No interaction detected  |  *** |   |  ***  |
| E                 | AerC  |  **  | n/d  | No interaction detected   | No interaction detected  |  *** |  *** |  ***  |
| F                 | CheA1 | n/d   |  ** | n/d   | No interaction detected  | n/d   | n/d   |  *** |
| G                 | CheW1 | n/d   | n/d  | No interaction detected   | n/d  | n/d   | Strong  |  *  |

**Figure 9. BACTH analysis testing for interactions of chemoreceptors Tlp1, Tlp4a, and AerC with CheA1, CheA4, CheW1, CheW4 chemotaxis proteins and with one another.** Formation of red colonies (above the negative control levels) signifies that protein-protein interaction occurs. \* - no interaction, \*\* - weak interaction, \*\*\* - strong interaction, n/d – not determined

The Tlp4a chemoreceptor is encoded within the *che4* operon and is predicted to interact with CheA4. It was found to weakly interact with CheA4 when these proteins were expressed from both high and low copy vectors suggesting that Tlp4a likely signals via Che4 pathway (1D and 4A). In addition, Tlp4a was found to strongly interact with CheW1, a coupling protein encoded within the *che1* operon (7D) when CheW1 was expressed from high copy vector. Yet, Tlp4a did not interact with CheA1 (Figure 10) suggesting that it may only signal through Che4 pathway.

AerC is a cytoplasmic chemoreceptor that affects reversal frequency controlled by the signaling output of the *che4* operon, suggesting that this soluble chemoreceptor interacts with proteins in the Che4 pathway such as CheA4 and CheW4 (Xie *et al.*, 2010; Kumar, 2012). AerC was found to weakly interact with CheA4 when expressed from both plasmids (5A and 1E) and CheW4 (5B) indicating that AerC does in fact interact with chemotaxis proteins in the Che4 pathway and likely signals via this pathway. It was previously found that AerC localizes to the cell pole in Che1-dependent manner, and is therefore predicted to interact with chemotaxis proteins in the Che1 pathway. Indeed, AerC strongly interacted with CheA1 and CheW1 (6E and 7E, Figure 10).

Altogether these data suggest that chemoreceptors Tlp1, Tlp4a, and AerC interact with chemotaxis proteins in the Che4 pathway and likely signal via the Che4. Moreover, AerC interacts with chemotaxis proteins from both Che1 and Che4 pathways and likely signals via both Che1 and Che4 providing additional evidence for the suggested cross-talk at the receptors level. In contrast to AerC, Tlp1 and Tlp4a preferentially interacted with CheA4, CheW4, and CheW1 (Tlp4a) but not CheA1 suggesting that they may only signal through Che4 pathway.



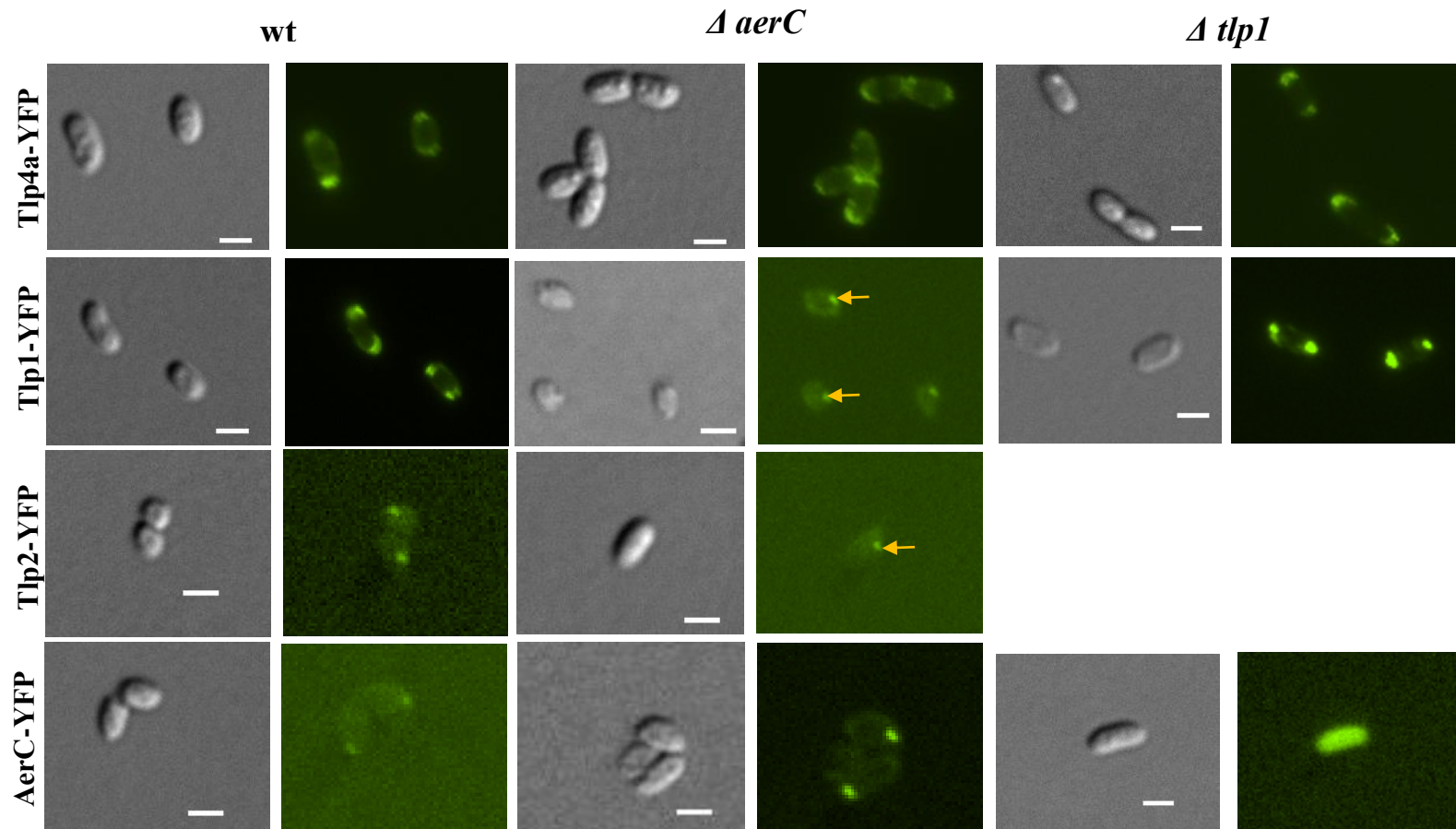
**Figure 10. Graphical representation of BACTH assay results depicting interactions of the chemoreceptors with chemotaxis proteins in the CheA1 and CheA4 pathways.**

### **Relative subcellular localization of chemoreceptors.**

In the model organism *E. coli*, chemoreceptors form mixed clusters, and the composition of each clusters depends on the relative expression level of individual chemoreceptor protein (Studdert and Parkinson 2003). However, it is unknown whether chemoreceptors in *A. brasilense* also form mixed clusters. We used fluorescent microscopy to investigate whether localization of Tlp1-YFP, Tlp4a-YFP, AerC-YFP, and Tlp2-YFP chemoreceptors is dependent upon the presence of the other receptors by evaluating their localization in the wild type (Sp7) and various mutant backgrounds.

In the wild type strain background, Tlp4a-YFP and Tlp1-YFP form tight clusters that localize to both cell poles (Figure 11). To evaluate whether Tlp1 and Tlp4a chemoreceptors depend on one another for proper localization, we determined the subcellular localization of Tlp4a-YFP in the  $\Delta tlp1$  background (Greer-Phillips *et al.*, 2004) and found that it localized similar to the wild type at the cell poles (Figure 15 and Figure 16). When relative fluorescence intensities of the polar foci were evaluated, we found that brightness of the Tlp4a-YFP foci was unaffected in the  $\Delta tlp1$  background compared to the wild type (p-value>0.05, Figure 12). In addition, Tlp4a-YFP expression was not affected in  $\Delta tlp1$  strain and appeared the same as in the wild type strain (Figure 8B). Altogether these data suggest that removal of Tlp1-YFP does not affect localization, expression, and cluster architecture of Tlp4a-YFP.





**Figure 11. Localization of chemoreceptors in respect to one another.** Fluorescent microscopy images of Tlp1-YFP and Tlp4a-YFP in the wild type and mutant backgrounds. The cells were grown to similar OD<sub>600</sub> and immobilized on 1% agarose pad in 1XPBS. Images were acquired after 2-3 hours on the pad (Tlp4a-YFP and Tlp1-YFP) or after 16-24 hrs (all strains expressing AerC-YFP). Orange arrows point at non-polar (mislocalized) foci, scale bars – 2 μm.

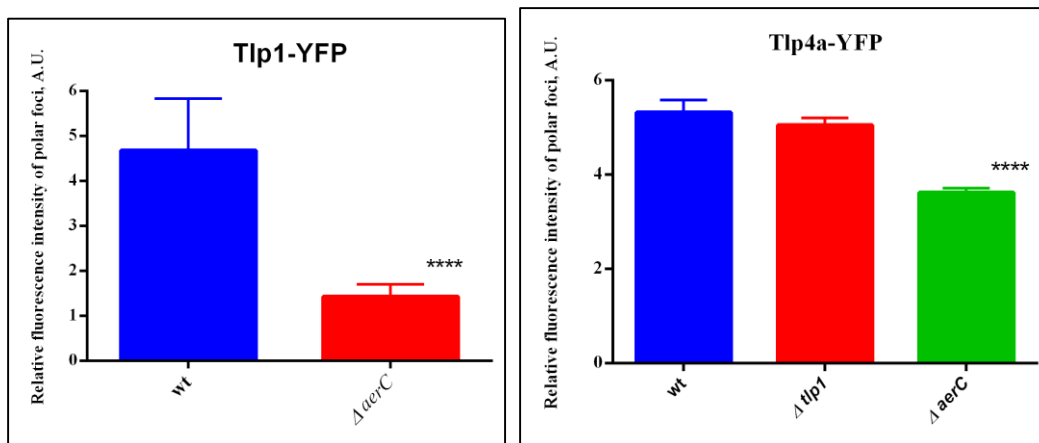
In order to evaluate whether localization of Tlp1, Tlp4a, and Tlp2 (Russell *et al.*, 2013), which is expected to signal similarly to Tlp1 (Russell *et al.*, 2013) depends on the presence of the cytoplasmic chemoreceptor AerC, we evaluated the localization of these chemoreceptors, expressed as fluorescent fusion to YFP, in the  $\Delta aerC$  strain. Tlp4a-YFP foci localized at the cell poles, mostly similar to the wild type (Figure 11, Figure 15, and Figure 16). However, they appeared more diffuse than the foci seen in the wild type background and formed a so-called “cap”. The average area that Tlp4a-YFP foci occupied in the wild type strain was  $3.2 \pm 1.6 \mu\text{m}^2$  while it was significantly larger in the  $\Delta aerC$  strain –  $10.3 \pm 5 \mu\text{m}^2$  (p-value < 0.0001, N=90). Also, relative fluorescence intensity of Tlp4a-YFP polar foci in the  $\Delta aerC$  strain was significantly lower than in the wild type strain (Figure 12, p-value < 0.001). However, when cellular levels of Tlp4a-YFP were evaluated using Western blotting, we found that expression of Tlp4a-YFP was only slightly lower in the  $\Delta aerC$  strain compared to the wild type strain suggesting that decrease in fluorescence intensity is not due to protein degradation but due to diffusion (Figure 13). These data suggest that removal of AerC does not have an effect on localization of Tlp4a-YFP but it may affect cluster structure since the size of the polar foci was much larger and relative fluorescence intensity of Tlp4a-YFP was decreased in the  $\Delta aerC$  background.

In contrast to Tlp4a-YFP, localization of both Tlp1-YFP and Tlp2-YFP was significantly affected in the  $\Delta aerC$  strain (Figure 11). First, the Tlp1-YFP clusters were not as bright as in the wild type (Figure 11 and Figure 12). Second, the majority of cells expressing Tlp1-YFP and Tlp2-YFP in the  $\Delta aerC$  background contained nonpolar fluorescent foci (Figure 15). The majority of the Tlp1-YFP and Tlp2-YFP fluorescent foci in this strain were also located on the

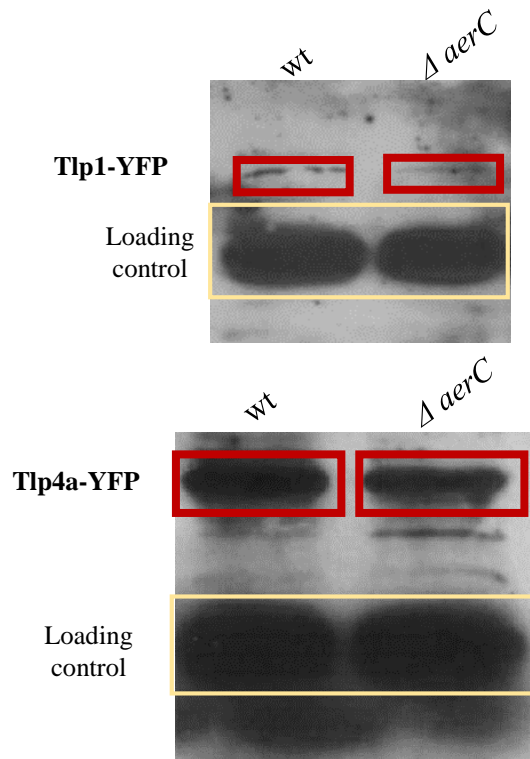
lateral sides of the cells or between the two cell poles, in contrast to the wild type's mostly polar localization of these foci (Figure 16). Similar to Tlp4a-YFP, fluorescence intensity of Tlp1-YFP foci was significantly decreased compared to the wild type (Figure 12, p-value<0.0001). Western blotting experiment results indicate that decreased fluorescence is due to protein degradation since Tlp1-YFP band was much fainter than the Tlp1-YFP in the wild type strain (Figure 13). Interestingly, the number of cells with mislocalized foci was not significantly different for the  $\Delta aerC$  (Tlp1-YFP) and  $\Delta aerC$  (Tlp2-YFP) strains (p-value>0.05), suggesting that *aerC* deletion has a similar effect on clusters where Tlp1 and Tlp2 are found, consistent with the proposed suggestion that Tlp2 signals in a Che1-dependent manner, similar to Tlp1 (Russell *et al.*, 2013).

Since AerC removal had such a drastic effect on localization of transmembrane chemoreceptors, we evaluated localization of AerC fused to YFP in the wild type,  $\Delta aerC$  (used as a control), and  $\Delta tlp1$  strains. AerC was found to localize to the cell poles in the wild type strain under nitrogen fixing conditions (low oxygen concentrations and no nitrogen present; Xie *et al.*, 2010). Therefore, all the strains expressing AerC-YFP were imaged under these conditions (nitrogen fixation was induced by leaving cells for 4-6 hours in minimal media lacking nitrogen source and then placing them on an agarose pad for 24 hours). In the  $\Delta aerC$  strain, AerC-YFP foci appeared as tight polar clusters; however, in the absence of Tlp1, AerC-YFP fluorescence was diffused indicating that AerC-YFP proteins were present in the cytoplasm but did not localize to the cell poles or formed clusters (Figure 11). When quantified, relative fluorescence intensity of AerC-YFP was significantly decreased in the  $\Delta tlp1$  background compared to the  $\Delta aerC$  (Figure 14, p-value<0.0001; diffused fluorescence is equal to 1 since fluorescence

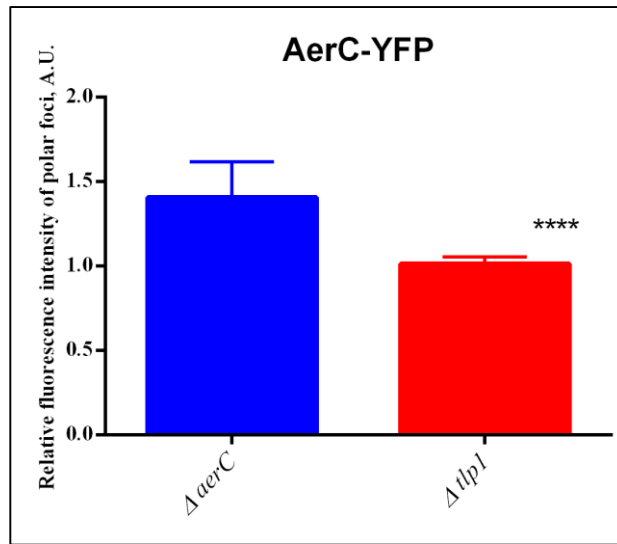
intensity at the pole is the same as in the cell body). Altogether our data suggest that AerC and Tlp1 are both implicated in chemotaxis receptor clustering. The fact that Tlp1-YFP formed clusters even in the absence of AerC, while AerC-YFP appeared diffused in the absence of Tlp1 may be explained by the fact that AerC is a soluble chemoreceptor that likely requires interaction with a transmembrane chemoreceptor (such as Tlp1) to localize to the cell pole.



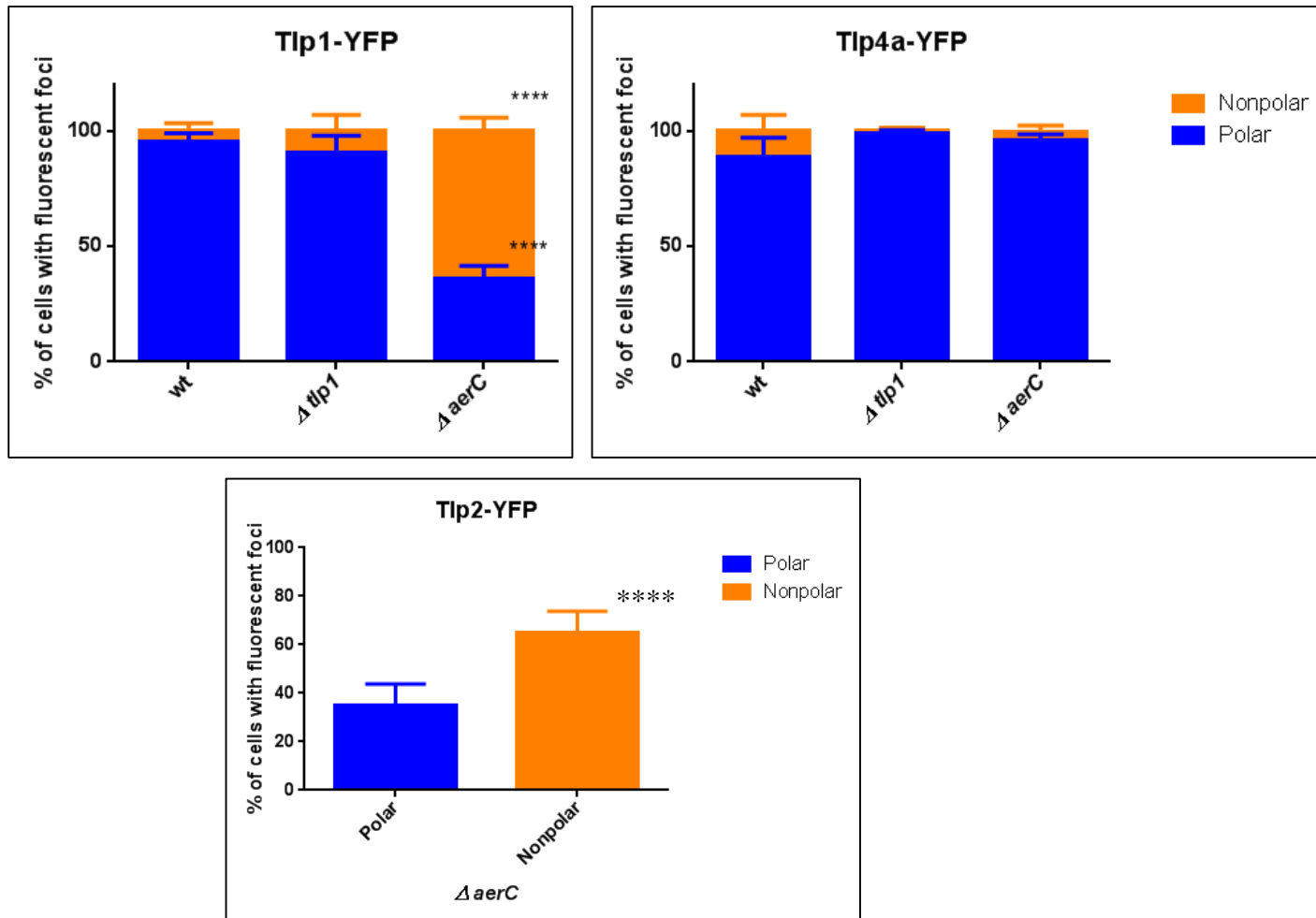
**Figure 12. Relative fluorescence intensity of Tlp4a-YFP and Tlp1-YFP is decreased in  $\Delta aerC$  background compared to the wild type.** Bar graphs depict fluorescence intensity of the polar foci relative to the fluorescence intensity of the cell body. All data are shown as mean +1SD.  $N \geq 80$  cells. \*\*\*\*-p-value $<0.0001$ .



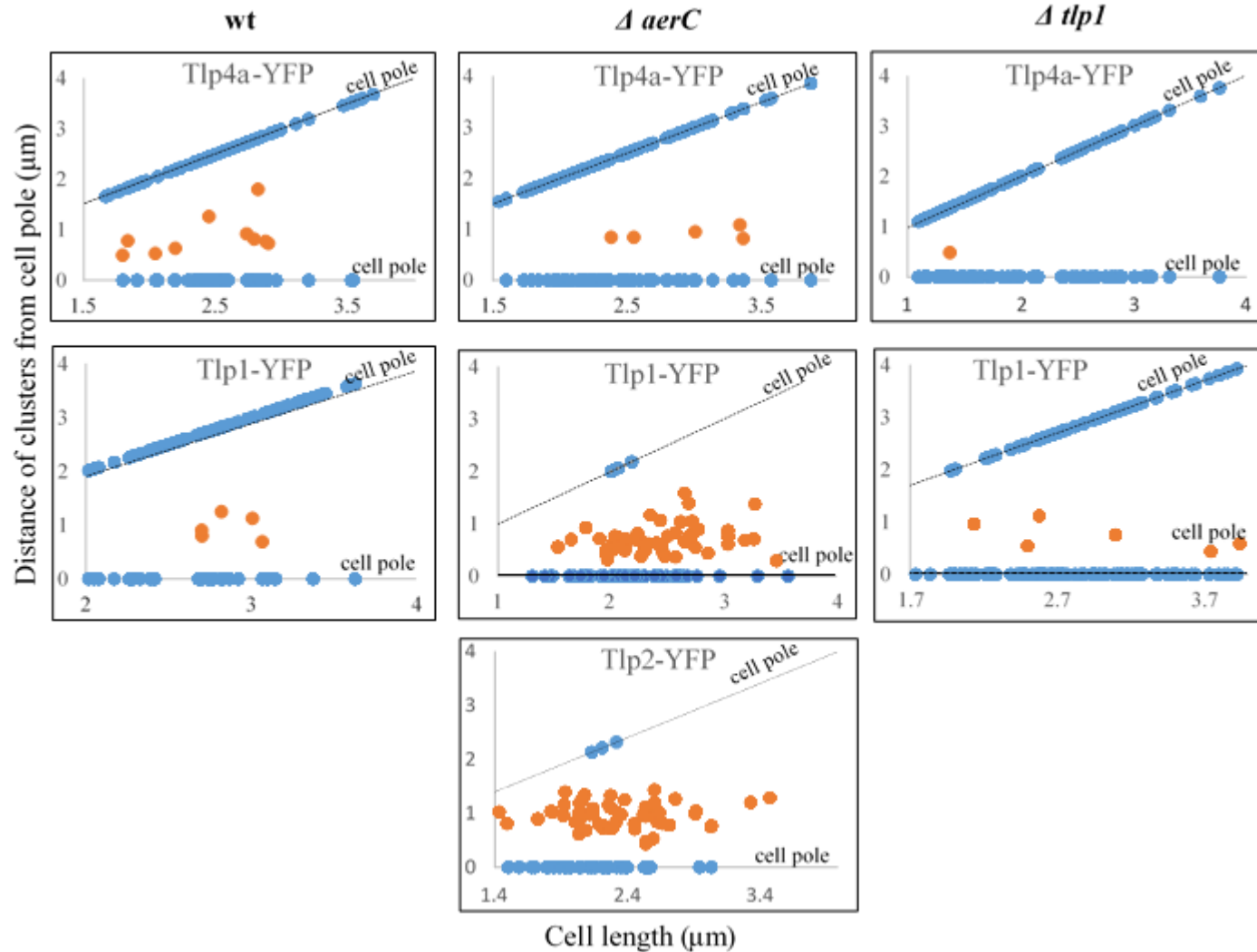
**Figure 13. Cellular levels of Tlp1-YFP and Tlp4a-YFP expressed from pRH005 plasmid.** Equivalent total protein concentrations were analyzed in all samples. Expression of Tlp1-YFP and Tlp4a-YFP from pRH005 plasmid was probed with anti-GFP primary antibody (1:1,000 dilution). Bands in red boxes are the bands corresponding to Tlp1-YFP (panel A) and Tlp4a-YFP (panel B). The bands in yellow boxes represent loading controls. Tlp1-YFP is degraded in the  $\Delta aerC$  strain while Tlp4a-YFP is slightly degraded in the  $\Delta aerC$  compared to the wild type.



**Figure 14. Relative fluorescence intensity of AerC-YFP is decreased in  $\Delta tlp1$  background compared to the  $\Delta aerC$  background.** Bar graphs depict fluorescence intensity of the polar foci relative to the fluorescence intensity of the cell body. All data are shown as mean +1SD.  $N \geq 80$  cells. \*\*\*\*- p-value < 0.0001.



**Figure 15. Localization of Tlp1-YFP and Tlp2-YFP is affected in the  $\Delta aerC$  background while Tlp4a-YFP localizes to the cell pole irrespective of the background.** Stacked bar graphs depict polar (blue) and nonpolar (orange) localization of Tlp1-YFP, Tlp4a-YFP, and Tlp2-YFP fluorescent foci. All data are shown as mean +1SD, \*\*\*\* - p-value<0.0001, N $\geq$ 80 cells.



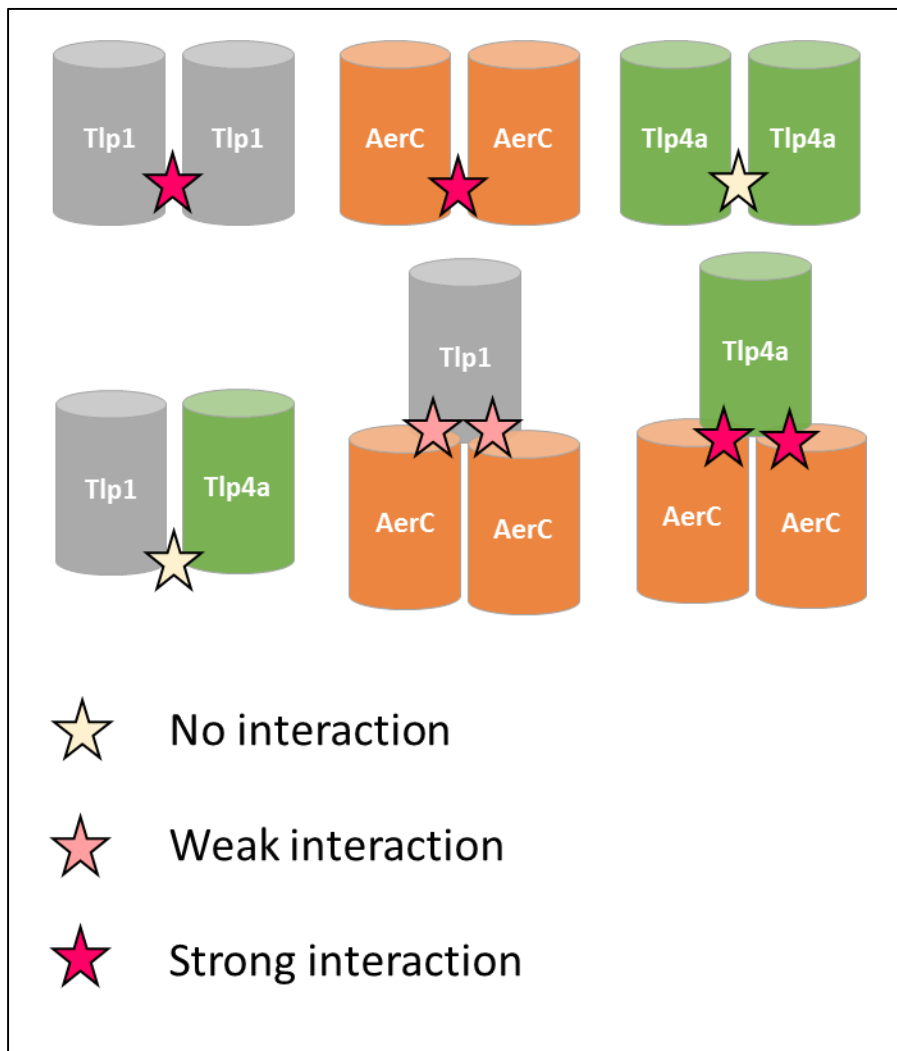
**Figure 16. Tlp1-YFP and Tlp2-YFP fluorescent foci are lateral in the  $\Delta aerC$  background while Tlp4a-YFP foci localize to the cell pole(s) in all backgrounds.** Graphs depict the distance of Tlp1-YFP, Tlp2-YFP, and Tlp4a-YFP clusters from the cell poles as a function of cell length (blue dots represent fluorescent foci at the pole, orange dots represent mislocalized foci).  $N \geq 80$  cells.



***In vivo* interactions of chemoreceptors with one another evaluated by Bacteria-Two Hybrid Assay.**

BACTH assay was used to elucidate protein-protein interactions among the receptors. Tlp1 was found to strongly interact with itself and AerC when the latter was present in excess (expressed from high copy vector) (Figure 9). AerC strongly interacted with itself and with Tlp4a when AerC was expressed from a high copy vector but not the other way around (Figure 17). Interactions of receptors with themselves can be explained by the fact that the basic unit of signaling (in *E. coli*) is receptors trimers-of-dimers in which receptors interact at their C-termini. Therefore, in *A. brasilense* chemoreceptors likely form trimers-of-dimers as well, hence the positive interactions. AerC only interacted with Tlp1 and Tlp4a when present in higher amount than the other two (expressed from a high copy plasmid). In contrast to AerC and Tlp1, Tlp4a did not interact with itself suggesting that Tlp4a may not dimerize and may require another chemoreceptor to form heterodimers. Finally, no interaction was detected between Tlp1 and Tlp4a in both vectors combinations consistent with fluorescent microscopy data described previously in this work ( $\Delta tlp1$  had no effect on Tlp4a-YFP localization or fluorescence intensity).

In conclusion, our data suggest that AerC interacts with both Tlp1 and Tlp4a chemoreceptors when present in excess but Tlp1 and Tlp4a do not interact with one another (Figure 17). Along with fluorescent imaging data it means that Tlp1 and Tlp4a may form mixed clusters with AerC. However, they are not likely to form mixed clusters with one another and possibly form two distinct clusters.



**Figure 17. Graphical representation of BACTH assay results depicting interactions of the chemoreceptors with one another.**

## CHAPTER IV. Discussion

In a model organism *E. coli*, chemoreceptors form mixed clusters and subsequently large arrays that localize to the cell poles along with the CheA histidine kinase and the CheW coupling protein as revealed by PALM (photoactivated localization microscopy), fluorescence microscopy, and cross-linking studies (Greenfield *et al.*, 2009; Kentner, 2006; Studdert and Parkinson, 2003). Cryo-ET studies of 13 distinct bacterial species showed that such architecture is universally conserved and likely contributes to signal gain and amplification (Briegel *et al.*, 2009). Interaction of chemoreceptors with the histidine kinase CheA is required for chemotaxis signaling but it appears not to be required for chemoreceptor cluster formation (Kentner *et al.*, 2006). In the absence of CheA in *E. coli*, chemoreceptors formed multiple lateral clusters and appeared diffused. In the absence of the coupling protein CheW, chemoreceptors clusters were localized at the cell poles,, but these clusters appeared less compact compared to the wild type clusters (Kentner *et al.*, 2006). Recent cryo-ET studies in *E. coli* confirmed that CheA and CheW proteins are not required for chemoreceptors cluster formation but that these proteins are essential for the formation of large receptor arrays found at the cell poles (Briegel *et al.*, 2014). Since more than half of the bacterial species which genomes have been sequenced, contain more than one CheA homologue, how multiple CheAs and numerous receptors organize within the cells and how the presence of these multiple proteins affect the formation of chemoreceptors clusters.

The genome of the alphaproteobacterium *A. brasilense* encodes for 41 chemoreceptors, and several CheA and CheW homologs (Wisniewsky-Dye *et al.*, 2012). Experiments performed to date indicate that *che1* and *che4* operons contribute to chemotaxis via an effect on swimming

speed (Bible *et al.*, 2008) and reversal frequency (Kumar, 2012; unpublished data). Additional data also hint at a potential signaling cross-talk during chemotaxis, which may be initiated at the receptors level (Stephens *et al.*, 2006; Russell *et al.*, 2013). Experimental evidence also suggest that several chemoreceptors in *A. brasilense* (Tlp1 and AerC) signal via both Che1 and Che4 (Xie *et al.*, 2010; Bible *et al.*, 2012; Russell *et al.*, 2013). Since *A. brasilense* has at least two CheAs interacting with chemoreceptors (CheA1 and CheA4) their effect on chemoreceptors cluster formation and localization is expected to be different from that described in *E. coli*. The observations made in *A. brasilense* and described above suggest several possibilities that are not mutually exclusive regarding the organization of chemoreceptor arrays within this bacterial species. One possibility is that distinct arrays cluster mixed sets of chemoreceptors, with one cluster dedicated to relay Che1 signals and another for Che4 signaling. Another possibility is that chemoreceptors are organized in a single large array that also interacts with both Che1 and Che4 proteins. Under both possibilities, the organization of chemoreceptors within the arrays and their interaction with Che1 and Che4 protein must be distinct to account for signal integration in chemotaxis and cross-talk signaling. In this study we elucidated organization of bacterial chemoreceptors in respect to one another and to chemotaxis proteins from Che1 and Che4 pathways using fluorescence microscopy and *in vivo* BACTH assay.

Until this study, the subcellular localization and organization of chemoreceptors from *A. brasilense* that belong to 5 different signaling domain classes was unknown. Based on the results of this study, we propose that Tlp1 and Tlp4a chemoreceptors belong to two distinct clusters (Figure 18). This is based on the fact that removal of Tlp1 does not affect Tlp4a localization, expression, and cluster formation. In addition, Tlp1 and Tlp4a were not found to interact *in vivo*.

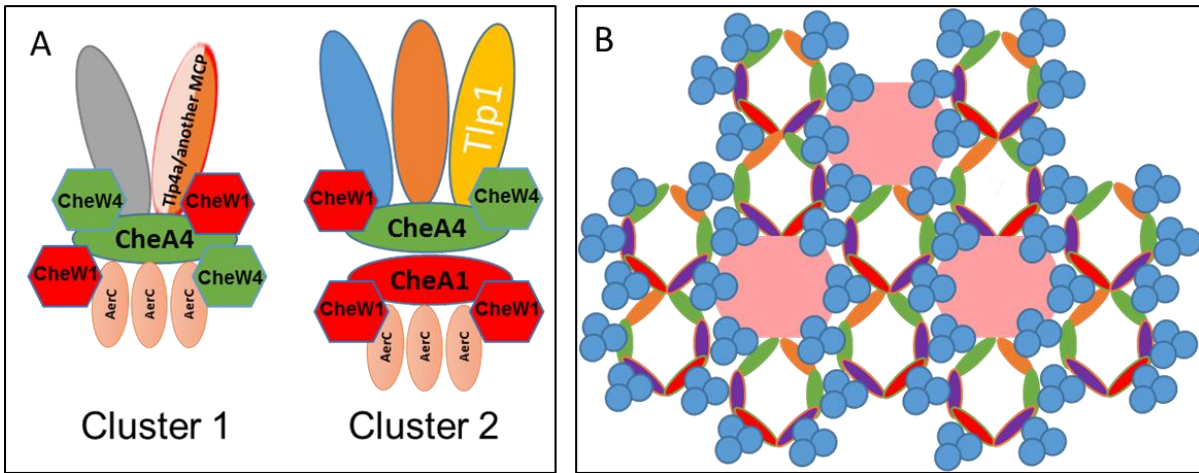
Finally, recent reports demonstrate that receptors from different signaling domain classes in *E. coli* (40H and 36H) do not intermix in clusters (Herrera Seitz *et al.*, 2014). Tlp1 (and 32 other chemoreceptors) belongs to the 38H class, while Tlp4a belongs to the 36H class; therefore, we propose that these two receptors (and other receptors from the same class) do not form mixed clusters and in fact likely belong to two physically distinct clusters.

Through fluorescence microscopy studies, we have found that chemoreceptors polar localization and recruitment to the clusters depends on the presence of CheA4. CheA4 was also found to be interacting with the receptors and both CheW1 and CheW4 *in vivo*. The later observation is significant because it provides a mechanistic rationale for the observed signaling cross-talk between the Che1 and Che4 pathways. CheA1 strongly interacted with AerC but it was not found to interact with Tlp1 or Tlp4a. Based on these evidence, we are proposing the following model for chemoreceptors clusters organization in *A. brasilense*. Cluster 1 is comprised of Tlp4a and the other two chemoreceptors belonging to the same signaling class, and it interacts with CheA4 and CheW4. Indeed we have found that Tlp4a weakly interacted, *in vivo*, with CheA4 and CheW4 (Figure 18). Tlp4a did not interact with CheW1, and could therefore be coupled to CheA4 only indirectly, likely through CheW4. CheA4 interacted with both CheW1 and CheW4; therefore, in this particular cluster, CheA4 may be coupled to the other receptors through CheW1. Since Tlp4a did not interact with itself *in vivo* (and likely does not form dimers), we are proposing that another chemoreceptor of the same signaling class dimerizes with Tlp4a to form heterodimers and thus permits signaling and cluster assembly. AerC was found to strongly interact with Tlp4a, and Tlp4a's cluster architecture was affected in the  $\Delta aerC$

background. Therefore, we propose that AerC is also present in Cluster 1 (on the cytoplasmic side).

The second cluster is comprised of the chemoreceptors belonging to the 38H class (such as Tlp1 and Tlp2) and interact with both CheA1 and CheA4. This is supported by the fact that polar localization of Tlp1 depends on the presence of CheA4, and that CheA4 and Tlp1 strongly interacted *in vivo*. Tlp1 did not interact with CheA1 or CheW1 *in vivo*, but it was found to signal via the Che1 pathway (Russell *et al.*, 2013). In addition, CheA1 and CheA4 were found to strongly interact *in vivo* and may form heterodimers. Therefore, we propose that Tlp1 relays signal through Che1 via interaction with CheA4-CheA1 heterodimers. Another possibility is that CheA1 may be present in Cluster 2 but does not physically interact with Tlp1 (Figure 18B). AerC was found to interact with Tlp1, CheA1, and CheW1 *in vivo* and to affect the localization of Tlp1 and Tlp2. AerC has also been previously shown to localize to the cell poles in a Che1-dependent manner (Xie *et al.*, 2010). Therefore, we hypothesize that this soluble chemoreceptor is present in Cluster 2. Our fluorescent microscopy results suggest that soluble chemoreceptor AerC has an effect on transmembrane chemoreceptor clustering since the absence of AerC affected localization of Tlp1/Tlp2 as well as the architecture of the Tlp4a cluster. To our knowledge, a similar effect of a soluble receptor on the localization of transmembrane chemoreceptors has not been reported.

In conclusion, our study reveals a novel mode of bacterial chemoreceptor organization in which transmembrane chemoreceptors form two distinct clusters that preferentially interact with one CheA (cluster 1) or both CheA1 and CheA4 (cluster 2) and in which a soluble chemoreceptor AerC plays a structural role in transmembrane chemoreceptor clustering.



**Figure 18. Model of chemoreceptors clusters organization in *A. brasilense*.**

## **LIST OF REFERENCES**



- Alexander, R. P., & Zhulin, I. B. (2007). Evolutionary genomics reveals conserved structural determinants of signaling and adaptation in microbial chemoreceptors. *Proceedings of the National Academy of Sciences of the United States of America*, *104*(8), 2885–90.
- Alexandre, G. (2010). Coupling metabolism and chemotaxis-dependent behaviors by energy taxis receptors. *Microbiology (Reading, England)*, *156*(8), 2283–93.
- Bai, F., Branch, R. W., Nicolau, D. V, Pilizota, T., Steel, B. C., Maini, P. K., & Berry, R. M. (2010). Conformational spread as a mechanism for cooperativity in the bacterial flagellar.
- Bibikov, S.I., Miller, A.C., Gosink, K.K., Parkinson. J.S. (2004) Methylation-independent aerotaxis mediated by the *Escherichia coli* Aer protein. *J Bacteriol*, *186*, 3730–3737.
- Bible, A. N., Stephens, B. B., Ortega, D. R., Xie, Z., & Alexandre, G. (2008). Function of a chemotaxis-like signal transduction pathway in modulating motility, cell clumping, and cell length in the alphaproteobacterium *Azospirillum brasilense*. *Journal of Bacteriology*, *190*(19), 6365–75.
- Bible, A. N. (2012) Characterization of the Function of the *Azospirillum brasilense* Che1 Chemotaxis Pathway in the Regulation of Chemotaxis, Cell Length and Clumping. PhD diss., University of Tennessee.
- Briegel, A., Ding, H., Li, Z., & Werner, J. (2008). Location and architecture of the *Caulobacter crescentus* chemoreceptor array. *Molecular Microbiology*, *69*(1), 30–41.
- Briegel, A., Ladinsky, M. S., Oikonomou, C., Jones, C. W., Harris, M. J., Fowler, D. J., Jensen, G. J. (2014). Structure of bacterial cytoplasmic chemoreceptor arrays and implications for chemotactic signaling. *eLife*, *3*, e02151.
- Briegel, A., Li, X., Bilwes, A. M., Hughes, K. T., Jensen, G. J., & Crane, B. R. (2012). Bacterial chemoreceptor arrays are hexagonally packed trimers of receptor dimers networked by rings of kinase and coupling proteins. *Proceedings of the National Academy of Sciences of the United States of America*, *109*(10), 3766–71.
- Briegel, A., Ortega, D. R., Tocheva, E. I., Wuichet, K., Li, Z., Chen, S., Jensen, G. J. (2009). Universal architecture of bacterial chemoreceptor arrays. *Proceedings of the National Academy of Sciences of the United States of America*, *106*(40), 17181–6.
- Briegel, A., Wong, M. L., Hodges, H. L., Oikonomou, C. M., Piasta, K. N., Harris, M. J., Jensen, G. J. (2014). New insights into bacterial chemoreceptor array structure and assembly from electron cryotomography. *Biochemistry*, *53*(10), 1575–85.

- Dobbelaere, S., & Okon, Y. (2007). *Associative and Endophytic Nitrogen-fixing Bacteria and Cyanobacterial Associations*. (C. Elmerich & W. E. Newton, Eds.) (Vol. 5, pp. 145 – 170). Dordrecht: Springer Netherlands.
- Duke, T. A., & Bray, D. (1999). Heightened sensitivity of a lattice of membrane receptors. *Proceedings of the National Academy of Sciences of the United States of America*, 96(18), 10104–8.
- Falke, J. J., Bass, R. B., Butler, S. L., Chervitz, S. A., & Danielson, M. A. (1997). The two-component signaling pathway of bacterial chemotaxis: a molecular view of signal transduction by receptors, kinases, and adaptation enzymes. *Annual review of cell and developmental biology*, 13, 457–512.
- Francis, N. R., Wolanin, P. M., Stock, J. B., Derosier, D. J., & Thomas, D. R. (2004). Three-dimensional structure and organization of a receptor/signaling complex. *Proceedings of the National Academy of Sciences of the United States of America*, 101(50), 17480–5.
- Gegner, J. A., Graham, D. R., Roth, A. F., & Dahlquist, F. W. (1992). Assembly of an MCP receptor, CheW, and kinase CheA complex in the bacterial chemotaxis signal transduction pathway. *Cell*, 70(6), 975–982.
- Greer-Phillips, S. E., Stephens, B. B., & Alexandre, G. (2004). An Energy Taxis Transducer Promotes Root Colonization by *Azospirillum brasilense*, 186(19), 6595–6604.
- Hallez, R., Letesson, J.-J., Vandenhaute, J., & De Bolle, X. (2007). Gateway-based destination vectors for functional analyses of bacterial ORFeomes: application to the Min system in *Brucella abortus*. *Applied and Environmental Microbiology*, 73(4), 1375–9. doi:10.1128/AEM.01873-06
- Hauwaerts, D., Alexandre, G., Das, S. K., Vanderleyden, J., & Zhulin, I. B. (2002). A major chemotaxis gene cluster in *Azospirillum brasilense* and relationships between chemotaxis operons in alpha-proteobacteria. *FEMS Microbiology Letters*, 208(1), 61–7. Retrieved from <http://www.ncbi.nlm.nih.gov/pubmed/11934495>
- Hazelbauer, G. L., Falke, J. J., & Parkinson, J. S. (2008). Bacterial chemoreceptors: high-performance signaling in networked arrays. *Trends in Biochemical Sciences*, 33(1), 9–19.
- Herrera Seitz, M. K., Frank, V., Massazza, D. A., Vaknin, A., & Studdert, C. A. (2014). Bacterial chemoreceptors of different length classes signal independently. *Molecular Microbiology*, 93(4), 814–22. doi:10.1111/mmi.12700

- Kovach, M. E., Elzer, P. H., Steven Hill, D., Robertson, G. T., Farris, M. A., Roop, R. M., & Peterson, K. M. (1995). Four new derivatives of the broad-host-range cloning vector pBBR1MCS, carrying different antibiotic-resistance cassettes. *Gene*, 166(1), 175–176.
- Kumar, D. (2012). Characterization of the Che4 Signal Transduction Pathway in Taxis Behaviors of *Azospirillum brasilense*. Master's Thesis. University of Tennessee.
- Lacal, J., García-Fontana, C., Muñoz-Martínez, F., Ramos, J.-L., & Krell, T. (2010). Sensing of environmental signals: classification of chemoreceptors according to the size of their ligand binding regions. *Environmental Microbiology*, 12(11), 2873–84.
- Ladant, D. and Ullmann, A. (1999). Bordetella pertussis adenylate cyclase: a toxin with multiple talents. *Trends Microbiol.* 7, 172-176.
- Letunic, I., Doerks, T., & Bork, P. (2012). SMART 7: recent updates to the protein domain annotation resource. *Nucleic Acids Research*, 40(Database issue), D302–5.
- Li, M., & Hazelbauer, G. L. (2005). Adaptational assistance in clusters of bacterial chemoreceptors. *Molecular Microbiology*, 56(6), 1617–26.
- Liu, J., Hu, B., Morado, D. R., Jani, S., Manson, M. D., & Margolin, W. (2012). Molecular architecture of chemoreceptor arrays revealed by cryoelectron tomography of *Escherichia coli* minicells. *Proceedings of the National Academy of Sciences of the United States of America*, 109(23), E1481–8.
- Maddock, J. R., & Shapiro, L. (2014). Location of the Polar Chemoreceptor Complex in *Escherichia coli*. *Cell*, 259(5102), 1717–1723.
- McNally, D. F., & Matsumura, P. (1991). Bacterial chemotaxis signaling complexes: formation of a CheA/CheW complex enhances autophosphorylation and affinity for CheY. *Proceedings of the National Academy of Sciences of the United States of America*, 88(14), 6269–73.
- Park, S.-Y., Borbat, P. P., Gonzalez-Bonet, G., Bhatnagar, J., Pollard, A. M., Freed, J. H., Crane, B. R. (2006). Reconstruction of the chemotaxis receptor-kinase assembly. *Nature Structural & Molecular Biology*, 13(5), 400–7.
- Parkinson, J. S. (2010). Signaling mechanisms of HAMP domains in chemoreceptors and sensor kinases. *Annual Review of Microbiology*, 64, 101–22.
- Porter, S., Wadhams, G., & Armitage, J. (2011). Signal processing in complex chemotaxis pathways. *Nature Reviews Microbiology*.

- Rebbapragada, A., Johnson, M. S., Harding, G. P., Zuccarelli, A. J., Fletcher, H. M., Zhulin, I. B., & Taylor, B. L. (1997). The Aer protein and the serine chemoreceptor Tsr independently sense intracellular energy levels and transduce oxygen, redox, and energy signals for *Escherichia coli* behavior. *Proceedings of the National Academy of Sciences of the United States of America*, *94*(20), 10541–6.
- Russell, M. H., Bible, A. N., Fang, X., Gooding, J. R., Campagna, S. R., Gomelsky, M., & Alexandre, G. (2013). Integration of the second messenger c-di-GMP into the chemotactic signaling pathway. *mBio*, *4*(2), e00001–13.
- Silverman, M., & Simon, M. (1976). Operon controlling motility and chemotaxis in *E. coli*. *Nature*, *264*(5586), 577–580.
- Simon, L. D., Randolph, B., Irwin, N., & Binkowski, G. (1983). Stabilization of proteins by a bacteriophage T4 gene cloned in *Escherichia coli*. *Proceedings of the National Academy of Sciences of the United States of America*, *80*(7), 2059–62.
- Sourjik, V., & Berg, H. C. (2002). Receptor sensitivity in bacterial chemotaxis.
- Sourjik, V., & Berg, H. C. (2004). Functional interactions between receptors in bacterial chemotaxis. *Nature*, *428*(March), 1–4.
- Sourjik, V., & Wingreen, N. S. (2012). Responding to chemical gradients: bacterial chemotaxis. *Current opinion in cell biology*, *24*(2), 262–8.
- Studdert, C. A., & Parkinson, J. S. (2004). Crosslinking snapshots of bacterial chemoreceptor squads. *Proceedings of the National Academy of Sciences of the United States of America*, *101*(7), 2117–22.
- Thiem, S. et al. (2007) Positioning of chemosensory clusters in *E. coli* and its relation to cell division. *EMBO J.* *26*, 1615–1623.
- Universidade Federal do Parana. (2013). Azospirillum brasilense FP2 Genome Sequence. Retrieved September 18, 2014, from <http://www.ncbi.nlm.nih.gov/bioproject/182105>
- Wadhams, G. H., & Armitage, J. P. (2004). Making sense of it all: bacterial chemotaxis. *Nature Reviews. Molecular Cell Biology*, *5*(12), 1024–37.
- Welch, M., Oosawa, K., Aizawa, S., & Eisenbach, M. (1993). Phosphorylation-dependent binding of a signal molecule to the flagellar switch of bacteria. *Proceedings of the National Academy of Sciences*, *90*(19), 8787–8791.

- Wisniewski-Dyé, F., Borziak, K., Khalsa-Moyers, G., Alexandre, G., Sukharnikov, L. O., Wuichet, K., & Zhulin, I. B. (2011). Azospirillum genomes reveal transition of bacteria from aquatic to terrestrial environments. *PLoS Genetics*, 7(12), e1002430.
- Wuichet, K., & Zhulin, I. B. (2010). Origins and diversification of a complex signal transduction system in prokaryotes. *Science Signaling*, 3(128), 50.
- Xie, Z., Ulrich, L. E., Zhulin, I. B., & Alexandre, G. (2010). PAS domain containing chemoreceptor couples dynamic changes in metabolism with chemotaxis. *Proceedings of the National Academy of Sciences of the United States of America*, 107(5), 2235–40.
- Zhang, P., Khursigara, C. M., Hartnell, L. M., & Subramaniam, S. (2007). Direct visualization of Escherichia coli chemotaxis receptor arrays using cryo-electron microscopy. *Proceedings of the National Academy of Sciences of the United States of America*, 104(10), 3777–81.

## **VITA**

Anastasia Aksenova (De Cerqueira) was born in Kaluga, Russia. She attended 17<sup>th</sup> Elementary, Middle, and High School which she graduated in 2001. She continued her education in French-Russian Institute of Business Administration where she received Bachelor's Degree in Business Administration. In 2005, Anastasia switched her professional interests to science. She moved to Knoxville, TN in June 2005 where she attended Pellissippi State Technical Community College. She graduated with Associate's Degree in Biology, and then got her Bachelor's Degree in Biochemistry from Maryville College (Maryville, TN) in 2011. She participated in a Summer Internship Program at Oak Ridge National Laboratory in 2008 that made her interested in a career in biological sciences. Anastasia was offered a graduate teaching position at the University of Tennessee in Knoxville in 2011 where she worked under Dr. Gladys Alexandre. She completed her Master's of Science Degree in Biochemistry, Cellular and Molecular Biology in 2014.